*DOI:*
10.7554/eLife.43996

*Document Version*
Peer reviewed version

# Homeostatic and tumourigenic activity of SOX2+ pituitary stem cells is controlled by the LATS/YAP/TAZ cascade

Emily J. Lodge[1,2], Alice Santambrogio[1,3], John P. Russell[1], Paraskevi Xekouki[1,4], Thomas S. Jacques[5], Randy L. Johnson[6], Selvam Thavaraj[7], Stefan R. Bornstein[2,3], Cynthia L. Andoniadou[1,3,*]

[1]Centre for Craniofacial and Regenerative Biology, Faculty of Dentistry, Oral & Craniofacial Sciences, King's College London, Floor 27 Tower Wing, Guy's Campus, London, SE1 9RT, United Kingdom

[2] Division of Diabetes & Nutritional Sciences, Faculty of Life Sciences & Medicine, King's College London, London SE1 1UL, United Kingdom

[3] Department of Medicine III, University Hospital Carl Gustav Carus, Technische Universität Dresden, Dresden 01307, Germany

[4] Department of Endocrinology, King's College Hospital NHS Foundation Trust, London, SE5 9RS, UK

[5] UCL GOS Institute of Child Health and Great Ormond Street Hospital for Children NHS Foundation Trust, London, WC1N 1EH, UK.

[6] Department of Cancer Biology, The University of Texas, MD Anderson Cancer Center, 1515 Holcombe Blvd., Houston, Texas 77030, USA.

[7] Centre for Oral, Clinical and Translational Sciences, Faculty of Dentistry, Oral & Craniofacial Sciences, King's College London, London SE1 9RT, UK.

* Corresponding author: Cynthia L. Andoniadou, cynthia.andoniadou@kcl.ac.uk Tel: +44 207 188 7389, Fax: +44 20 7188 1674

**ABSTRACT**

SOX2 positive pituitary stem cells (PSCs) are specified embryonically and persist throughout life, giving rise to all pituitary endocrine lineages. We have previously shown the activation of the STK/LATS/YAP/TAZ signalling cascade in the developing and postnatal mammalian pituitary. Here, we investigate the function of this pathway during pituitary development and in the regulation of the SOX2 cell compartment. Through loss- and gain-of-function genetic approaches, we reveal that restricting YAP/TAZ activation during development is essential for normal organ size and specification from SOX2+ PSCs. Postnatal deletion of LATS kinases and subsequent upregulation of YAP/TAZ leads to uncontrolled clonal expansion of the SOX2+ PSCs and disruption of their differentiation, causing the formation of non-secreting, aggressive pituitary tumours. In contrast, sustained expression of YAP alone results in expansion of SOX2+ PSCs capable of differentiation and devoid of tumourigenic potential. Our findings identify the LATS/YAP/TAZ signalling cascade as an essential component of PSC regulation in normal pituitary physiology and tumourigenesis.

Key words: pituitary stem cell, SOX2, Hippo, YAP, pituitary tumour

## INTRODUCTION

SOX2 is crucial transcription factor involved in the specification and maintenance of multiple stem cell populations in mammals. Pituitary stem cells express SOX2 and contribute to the generation of new endocrine cells during embryonic development and throughout postnatal life[1, 2]. The pituitary gland is composed of three parts, the anterior, intermediate and posterior lobes (AL, IL and PL, respectively). The AL and IL contain hormone-secreting cells, which are derived from an evagination of the oral ectoderm expressing SOX2, termed Rathke's pouch (RP). SOX2+ cells, both in the embryonic and adult pituitary, can differentiate into three endocrine cell lineages, which are marked by transcription factors PIT1 (POU1F1)[3], TPIT (TBX19)[4] and SF1 (NR5A1)[5], and differentiate into hormone-secreting cells (somatotrophs, lactotrophs, thyrotrophs, corticotrophs, melanotrophs and gonadotrophs, which express growth hormone, prolactin, thyrotropin, adrenocorticotropin, melanotropin and gonadotropin, respectively). SOX2+ PSCs are highly proliferative during the first 2-3 weeks of life, in concordance with major organ growth, after which they reach a steady low proliferative capacity that contributes to maintain normal homeostasis and physiological adaptation of the pituitary gland[6, 7].

Contrary to other organs, where somatic stem cells are shown to be able to become transformed into cancer stem cells, the roles of SOX2+ PSCs in tumourigenesis remain poorly understood, possibly due to the patchy knowledge of the pathways regulating SOX2+ PSC fate and proliferation. Pituitary tumours are common in the population, representing 10-15% of all intracranial neoplasms[8, 9]. Adenomas are the most common adult pituitary tumours, classified into functioning, when they secrete one or more of the pituitary hormones, or non-functioning if they do not secrete hormones. In children, adamantinomatous craniopharyngioma (ACP) is the most common pituitary tumour. Targeting oncogenic beta-catenin in SOX2+ PSCs in the mouse generates clusters of senescent SOX2+ cells that induce tumours resembling ACP in a paracrine manner, i.e. the tumours do not derive from the targeted SOX2+ PSCs[1, 10]. Up to 15% of adenomas and 50% of ACP display aggressive behaviour with invasion of nearby structures including the hypothalamus and visual tracts, associated with significant morbidity and mortality[11]. Pituitary carcinomas exhibiting metastasis are rare but can develop from benign tumours[12, 13, 14]. Whether SOX2+ cells can cell autonomously contribute to pituitary neoplasia has not been hitherto demonstrated.

The Hippo pathway controls stem cell proliferation and tumourigenesis in several organs such as in the liver[15, 16], intestines[17] and lung[18, 19]. In the core phosphorylation cascade, STK3/4 kinases phosphorylate and activate LATS1/2 serine/threonine-protein kinases, which in turn phosphorylate co-activators Yes-associated protein (YAP1, a.k.a. YAP) and WW domain-containing transcription regulator protein 1 (WWTR1, a.k.a. TAZ) that are subsequently inactivated through degradation and cytoplasmic retention[20]. Active YAP/TAZ associate with TEAD transcription factors,

promoting the transcription of target genes such as *Cyr61* and *Ctgf*[21, 22, 23]. YAP/TAZ have been shown to promote proliferation and the stem cell state in several organs, and can also lead to transformation and tumour initiation when overexpressed[24, 25, 26]. The involvement of YAP/TAZ in the function of tissue-specific SOX2+ stem cells during development and homeostasis has not been shown. We previously reported strong nuclear localisation of YAP and TAZ exclusively in SOX2+ stem cells of developing Rathke's pouch and the postnatal anterior pituitary of mice and humans, and enhanced expression in human pituitary tumours composed of uncommitted cells, including ACPs and null-cell adenomas[27, 28], which do not express any of the lineage transcription factors PIT1, TPIT or SF1. In these populations we detected phosphorylation of YAP at serine 127 (S127) indicating LATS kinase activity. Together these point to a possible function for LATS/YAP/TAZ in normal pituitary stem cells and during tumourigenesis. Here, we have combined genetic and molecular approaches to reveal that deregulation of the pathway can promote and maintain the SOX2+ PSC fate under physiological conditions and that major disruption of this axis transforms SOX2+ PSCs into cancer-initiating cells giving rise to aggressive tumours.

## RESULTS

### Sustained conditional expression of YAP during development promotes SOX2+ PSC fate

To determine if YAP and TAZ function during embryonic development of the pituitary, we used genetic approaches to perform gain- and loss-of-function experiments. We first expressed a constitutive active form of YAP(S127A) using the *Hesx1-Cre* driver, which drives *Cre* expression in Rathke's pouch (RP) and the

hypothalamic primordium from 9.5dpc, regulated by administration of doxycycline through the reverse tetracycline-dependent transactivator (rtTA) system (*R26*$^{rtTA/+}$; see Methods for details, Scheme Fig1A). Analyses were restricted to embryonic time points. As expected, we confirmed accumulation of total YAP protein but not of TAZ or pYAP(S127), throughout the developing pituitary and hypothalamus of *Hesx1*$^{Cre/+}$*;R26*$^{rtTA/+}$*;Col1a1*$^{tetO\text{-}Yap/+}$ (hereafter YAP-TetO) embryos at 15.5dpc, but not of *Cre*-negative controls (Fig1B, Figure 1 – figure supplement 1A). Likewise, the YAP downstream target *Cyr61* (Fig1B) was also upregulated. Morphologically, YAP-TetO mutants displayed a dysplastic anterior pituitary, which was more medially compacted and lacked a central lumen, making it difficult to distinguish between the developing anterior and intermediate lobes (Fig 1C). Immunofluorescence staining against SOX2 at 15.5dpc demonstrated loss of SOX2 in the most lateral regions of control pituitaries (arrows in Fig. 1C), where cells are undergoing commitment; yet mutant pituitaries had abundant SOX2 positive cells in the most lateral regions (arrowheads in Fig1C). Immunostaining for LHX3, which is expressed in the developing anterior pituitary[29], was used to demarcate AL and IL tissue. Staining using antibodies against lineage markers PIT1, TPIT and SF1 revealed a concomitant reduction in committed cell lineages throughout the gland (Fig1D; PIT1 0.35% in mutants compared with 30.21% in controls (Student's t-test $P<0.0001$, n=3 for each genotype), TPIT 1.03% in mutants compared with 9.81% in controls (Student's t-test $P=0.0012$, n=3 for each genotype), SF1 0.34% in mutants compared with 4.14% in controls (Student's t-test $P=0.0021$, n=3 for each genotype)). We therefore conclude that sustained activation of YAP prevents lineage commitment and is sufficient to maintain the progenitor state during embryonic development.

We did not obtain any live *Hesx1*$^{Cre/+}$;*R26*$^{rtTA/+}$;*Col1a1*$^{tetO\text{-}Yap/+}$ pups at birth when treated with doxycycline from 5.5dpc (n=5 litters). To bypass the embryonic lethality of these early inductions, we commenced doxycycline treatment from 9.5dpc, the onset of RP formation (Figure 1 – figure supplement 1B). *Hesx1*$^{Cre/+}$;*R26*$^{rtTA/+}$;*Col1a1*$^{tetO\text{-}Yap/+}$ pups were viable and were maintained on doxycycline until P24, at which point the experimental end point was reached due to excessive weight loss and animals had to be culled following UK Home Office Regulations. Histological analyses of pituitaries revealed multiple anterior lobe cysts per gland, localising predominantly in the ventral AL (n=4) (Figure 1 – figure supplement 1C). These structures developed in YAP-accumulating regions and were lined by SOX2+ cells (Figure 1 – figure supplement 1D). The proportion of SOX2+ cells throughout the AL was increased, as was the percentage of SF1+ cells, whereas PIT1+ cell numbers were significantly decreased and the TPIT lineage, identified by ACTH antibody staining, was unaffected (Figure 1 – figure supplement 1E). The total number of cycling Ki-67+ cells showed a trend towards a decrease in *Hesx1*$^{Cre/+}$;*R26*$^{rtTA/+}$;*Col1a1*$^{tetO\text{-}Yap/+}$ mutants relative to controls, which did not reach significance (Figure 1 – figure supplement 1F). The cystic structures observed in *Hesx1*$^{Cre/+}$;*R26*$^{rtTA/+}$;*Col1a1*$^{tetO\text{-}Yap/+}$ mutants were reminiscent of Rathke's cleft cyst (RCC), which is a benign developmental anomaly of the pituitary characterised by the presence of ciliated and secretory cells, expression cytokeratins and frequent expression of p63. Immunostaining revealed that cysts were lined by cytokeratin+ cells using the AE1/AE3 pan-cytokeratin cocktail and basal cells were positive for nuclear p63 in *Hesx1*$^{Cre/+}$;*R26*$^{rtTA/+}$;*Col1a1*$^{tetO\text{-}Yap/+}$ mutant pituitaries (Figure 1 – figure supplement 1G). Staining using antibodies against ARL13B and Acetylated α-Tubulin (Lys40) marking cilia, revealed multi-ciliated cells along the cyst lining

178 (Figure 1 – figure supplement 1H). Combined staining using Alcian Blue and the
179 Periodic Acid-Schiff technique (AB/PAS) to recognise mucins, detected royal blue-
180 stained mucous cells lining the cysts (Figure 1 – figure supplement 1H). Taken
181 together, we conclude that sustained activation of YAP during embryonic and
182 postnatal pituitary development, promotes maintenance and abnormal expansion of
183 SOX2+ epithelia during development, resulting in the formation of cysts that
184 resemble RCC.
185
186 Next, we generated embryos null for TAZ and conditionally lacking YAP in the
187 *Hesx1* expression domain (Figure 1 – figure supplement 2A-E).
188 $Hesx1^{Cre/+};Yap^{fl/fl};Taz^{-l-}$ double mutants were obtained at expected ratios during
189 embryonic stages until 15.5dpc, however the majority of $Taz^{-/-}$ mutants with or
190 without compound *Yap* deletions showed lethality at later embryonic and early
191 postnatal stages[30] (Supplementary File 1). The developing pituitary gland of
192 $Hesx1^{Cre/+};Yap^{fl/fl};Taz^{-l-}$ double mutants appeared largely normal at 13.5dpc by
193 histology (Figure 1 – figure supplement 2A). Immunostaining against SOX2 to mark
194 embryonic progenitors and postnatal stem cells did not reveal differences in the
195 spatial distribution of SOX2+ cells between double mutants compared to controls
196 ($Hesx1^{+/+};Yap^{fl/fl};Taz^{+/+}$ and $Hesx1^{+/+};Yap^{fl/fl};Taz^{+/-}$) at 13.5dpc, 16.0dpc (Figure 1 –
197 figure supplement 2B) or P28, even in regions devoid of both TAZ and active YAP
198 (Figure 1 – figure supplement 2C,D). This suggests that YAP/TAZ are not required
199 for SOX2+ cell specification or survival. Likewise, analysis of commitment markers
200 PIT1and SF1 as well as ACTH to identify the TPIT lineage, did not show any
201 differences between genotypes (Figure 1 – figure supplement 2E). Together, these
202 data suggest there is no critical requirement for YAP and TAZ during development

for the specification of SOX2+ cells or lineage commitment, but that YAP functions to promote the SOX2 cell identity.

**LATS, but not STK, kinases are required for normal pituitary development and differentiation**

Since sustained activation of YAP led to an embryonic phenotype, we reasoned that YAP/TAZ need to be regulated during embryonic development. To determine if STK and LATS kinases are important in YAP/TAZ regulation we carried out genetic deletions in the pituitary.

Conditional deletion of *Stk3* and *Stk4* (also called *Mst2* and *Mst1*) in *Hesx1*$^{Cre/+}$;*Stk3*$^{fl/fl}$;*Stk4*$^{fl/fl}$ embryos did not lead to a pituitary phenotype (Figure 2 – figure supplement 1). A reduction of over 75% in total STK3/4 proteins in mutants was confirmed by western blot on total lysates from *Stk3*$^{fl/fl}$;*Stk4*$^{fl/fl}$ controls and *Hesx1*$^{Cre/+}$;*Stk3*$^{fl/fl}$;*Stk4*$^{fl/fl}$ mutants (Figure 2 – figure supplement 1B). Mutant pituitaries were macroscopically normal at birth (Figure 2 – figure supplement 1A), and showed comparable expression patterns of TAZ, YAP, pYAP to controls lacking *Cre*, without distinct accumulation of YAP or TAZ (Figure 2 – figure supplement 1C). The distribution of SOX2+ cells was comparable between mutants and controls (Figure 2 – figure supplement 1C). Normal lineage commitment was evident by immunofluorescence staining for PIT1, TPIT and SF1 at P10 (Figure 2 – figure supplement 1D). Mutant animals remained healthy and fertile until P70, at which point pituitaries appeared histologically normal (Figure 2 – figure supplement 1E). Since deletion of *Stk3/4* at embryonic stages does not affect embryonic or postnatal pituitary development, we conclude these kinases are not critical for YAP/TAZ

228 regulation in the pituitary.

229

230 We next focused on perturbing LATS kinase function, as we have previously shown
231 strong expression of *Lats1* in the developing pituitary and postnatal kinase activity in
232 SOX2+ stem cells[27]. However, *Hesx1*$^{Cre/+}$;*Lats1*$^{fl/fl}$ embryos showed unaffected
233 pituitary development and normal localisation and levels of YAP and TAZ as
234 assessed by immunofluorescence (Figure 2 – figure supplement 2A,B) when
235 compared with controls. mRNA *in situ* hybridisation against *Lats2* at P2, revealed
236 abundant *Lats2* transcripts upon conditional deletion of *Lats1*, suggesting a
237 compensatory upregulation of *Lats2* in the absence of LATS1 (Figure 2 – figure
238 supplement 2C), similar to previous reports of elevated YAP/TAZ signalling inducing
239 *Lats2* expression[31].

240

241 To overcome potential functional redundancy, we deleted both *Lats1* and *Lats2* in RP.
242 Deletion of *Lats2* alone (*Hesx1*$^{Cre/+}$;*Lats2*$^{fl/fl}$), did not reveal any developmental
243 morphological anomalies (Figure 2 – figure supplement 2D) and pups were identified
244 at normal Mendelian proportions (Supplementary File 2). Similarly, deletion of any
245 three out of four *Lats* alleles did not affect pituitary development and were identified
246 at normal ratios, similar to other tissues[32]. Homozygous *Hesx1*$^{Cre/+}$;*Lats1*$^{fl/fl}$;*Lats2*$^{fl/fl}$
247 mutants were identified at embryonic stages at reduced Mendelian ratios and were
248 absent at P0-P2, suggesting embryonic and perinatal lethality (Supplementary File 2).

249

250 Haematoxylin/eosin staining of the developing pituitary gland in
251 *Hesx1*$^{Cre/+}$;*Lats1*$^{fl/fl}$;*Lats2*$^{fl/fl}$ mutants revealed overgrowth of RP by 13.5dpc compared
252 to controls lacking *Cre* (Fig2A, n=4). Total TAZ and YAP proteins accumulated

throughout the developing gland in double mutants (arrowheads) but only in the SOX2+ periluminal epithelium of controls (arrows). The same regions showed a marked reduction in pYAP-S127 staining, which is observed in SOX2+ cells of the control (Fig2A). These findings are in line with LATS1/2 normally regulating YAP and TAZ in the pituitary and demonstrate successful deletion in RP. The mutant pituitary was highly proliferative (Fig2B, Figure 2 – figure supplement 2F; Ki-67 index average 47.42% ±1.73 SEM in control versus 76.04% ±9.11 SEM in the double mutant, $P$=0.0067, Student's $t$-test) and the majority of cells expressed SOX2 (Fig2A,C) but not SOX9 (Fig2B, Figure 2 – figure supplement 2F).

By 15.5dpc the pituitary was grossly enlarged and exerting a mass effect on the brain, had cysts and displayed areas of necrosis (asterisks Fig2, Figure 2 – figure supplement 2E, n=5). Staining for Endomucin to mark blood vessels revealed poor vascularisation in $Hesx1^{Cre/+};Lats1^{fl/fl};Lats2^{fl/fl}$ mutants compared to the ample capillaries seen in the control (Fig2C), which may account for the necrosis. This could be due to a direct inhibition of vascularisation or a consequence of the rapid growth of this embryonic tumour. We frequently observed ectopic residual pituitary tissue at more caudal levels, reaching the oral epithelium and likely interfering with appropriate fusion of the sphenoid, similar to other phenotypes involving pituitary enlargement (arrows Fig2C)[33, 34, 35]. Immunofluorescence to detect active (non-phosphorylated) YAP revealed abundant staining throughout the pituitary at 15.5dpc, compared to the control where active YAP localises in the SOX2 epithelium (Fig2C). Immunofluorescence using specific antibodies against lineage commitment markers PIT1, TPIT and SF1 at 15.5dpc revealed very few cells expressing PIT1, TPIT and SF1 in the double mutant (Fig2D; PIT1 9.14% in mutants compared with 51.4% in

controls (Student's *t*-test $P<0.0001$); TPIT 4.0% in mutants compared with 11.4% in controls (Student's *t*-test $P<0.007$); SF1 2.1% in mutants compared with 6.5% in controls (Student's *t*-test $P>0.05$) n=3 mutants and 5 controls), suggesting failure to commit into the three lineages. These data suggest that the LATS/YAP/TAZ axis is required for normal embryonic development of the anterior pituitary and that LATS1/2 kinases control proliferation of SOX2+ progenitors and their progression into the three committed lineages.

**Loss of LATS kinases results in carcinoma-like murine tumours**

Postnatal analysis of *Hesx1*$^{Cre/+}$;*Lats1*$^{fl/fl}$ pituitaries revealed that by P56, despite developing normally during the embryonic period, all glands examined exhibited lesions of abnormal morphology consisting of overgrowths, densely packed nuclei and loss of normal acinar architecture (n=15). To minimise the likely redundancy by LATS2 seen at embryonic stages, we generated *Lats1* mutants additionally haploinsufficient for *Lats2* (*Hesx1*$^{Cre/+}$;*Lats1*$^{fl/fl}$;*Lats2*$^{fl/+}$). These pituitaries also developed identifiable lesions accumulating YAP and TAZ (Figure 3 – figure supplement 1A), which were observed at earlier time points (P21 n=4), the earliest being 10 days, indicating increased severity. The number of lesions observed per animal was similar between the two models at P56 (3-8 per animal). Deletion of *Lats2* alone (*Hesx1*$^{Cre/+}$;*Lats2*$^{fl/fl}$), which is barely expressed in the wild type pituitary, did not result in any defects (Figure 3 – figure supplement 1B). We focused on the *Hesx1*$^{Cre/+}$;*Lats1*$^{fl/fl}$;*Lats2*$^{fl/+}$ double mutants for further analyses.

Histological examination of *Hesx1*$^{Cre/+}$;*Lats1*$^{fl/fl}$;*Lats2*$^{fl/+}$ pituitaries confirmed the abnormal lesions were tumours, characterised by frequent mitoses, focal necrosis, and

303 a focal squamous differentiation, as well as the occasional presence of cysts (Fig3A).
304 These lesions were identical to those in *Hesx1*$^{Cre/+}$;*Lats1*$^{fl/fl}$ pituitaries (not shown).
305 These tumours accumulated YAP/TAZ and upregulated expression of targets *Cyr61*
306 and *Ctgf* (Fig3B), confirming the validity of the genetic manipulation (Fig3B).
307 Tumours were also frequently observed in the anterior and intermediate lobe (Figure
308 3 – figure supplement 1C). Analysis of proliferation by Ki-67 immunostaining
309 revealed an elevated mitotic index of 7-28% in tumours (mean 15.46, SEM ±2.74),
310 compared to 2.97% (SEM ±1.2) mean in control pituitaries not carrying the *Lats1*
311 deletion (Fig3C).
312 In keeping with the morphological evidence of epithelial differentiation (Fig3A), the
313 tumours were positive for cytokeratins using AE1/AE3 (multiple keratin cocktail)
314 (Figure 3 – figure supplement 1E). Furthermore, the tumours showed focal
315 morphological evidence of squamous differentiation and showed positive nuclear p63
316 staining, frequently expressed in squamous carcinomas (Figure 3 – figure supplement
317 1E). In contrast, the tumours did not show immunohistochemical evidence of
318 adenomas i.e. negative for neuroendocrine markers, which all types of adenomas are
319 typically positive for: the neuroendocrine marker synaptophysin and neuron-specific
320 enolase (Figure 3 – figure supplement 1F). The lesions were also negative for
321 chromogranin A, a neuroendocrine granule marker often expressed in clinically non-
322 functioning pituitary adenomas. Tumours were also negative for vimentin, expressed
323 by spindle cell oncocytoma, an uncommitted posterior pituitary tumour (Figure 3 –
324 figure supplement 1F). Moreover, immunostaining against PIT1, TPIT and SF1
325 showed only sparse positive cells within the lesions, suggesting lack of commitment
326 into endocrine precursors and supporting the undifferentiated nature of the tumour
327 cells (Fig3D). Consistent with a tumourigenic phenotype, and role for LATS1

genomic stabilisation[36], staining for gamma-H2A.X detected elevated DNA damage in cells of the mutant pituitaries compared with controls (Figure 3 – figure supplement 1D). The absence of adenoma or oncocytoma markers together with the histological appearance, observation of focal necrosis and a high mitotic index support the features of squamous carcinoma.

**SOX2 +ve cells are the cell of origin of the tumours**

Tumour regions were mostly composed of SOX2 positive cells, a sub-population of which also expressed SOX9 (Fig3E, Figure 3 - figure supplement 1A; 85-97% of cells, 7 tumours across 4 pituitaries). Close examination of the marginal zone epithelium, a major SOX2+ stem cell niche of the pituitary, revealed a frequent 'ruffling' resembling crypts, likely generated through over-proliferation of the epithelial stem cell compartment (Fig3F). To determine if the cell of origin of the tumourigenic lesions is a deregulated SOX2+ stem cell, we carried our specific deletion of LATS1/2 in postnatal SOX2+ cells using the tamoxifen-inducible *Sox2-CreERT2* driver, combined with conditional expression of membrane-GFP in targeted cells ($Sox2^{CreERT2/+}$;$Lats1^{fl/fl}$;$Lats2^{fl/+}$;$R26^{mTmG/+}$).

Tamoxifen induction at P5 or P21, led to abnormal lesions in the anterior pituitary within three months in all cases. We focused our analyses on inductions performed at P5, from which time point all animals developed lesions by P35 (Fig4A). Similar to observations in $Hesx1^{Cre/+}$;$Lats1^{fl/fl}$;$Lats2^{fl/+}$ animals, these areas strongly accumulated YAP and TAZ (Fig4B), activated expression of targets *Cyr61* and *Ctgf*, displayed ruffling of the AL epithelium (Fig4C, Figure 4 – figure supplement 1E) and lacked lineage commitment markers (Fig4D, Figure 4 – figure supplement 1A). These

lesions showed a similar marker profile to *Hesx1-Cre*-targeted tumours, with positive p63 and AE1/AE3 staining (Figure 4 – figure supplement 1B). Lineage tracing confirmed expression of membrane GFP in tumourigenic lesions, characterised by the accumulation of YAP and expansion of SOX2+ cells, suggesting they were solely derived from SOX2+ cells (Fig4E, Figure 4 – figure supplement 1C). Taken together, our data support that LATS kinase activity is required to regulate the pituitary stem cell compartment. Loss of LATS1 is sufficient to drive deregulation of SOX2+ pituitary stem cells, generating highly proliferative non-functioning tumours with features of carcinomas.

**YAP expression is sufficient to activate pituitary stem cells.**

Conditional deletion of LATS1/2 kinases in the pituitary has revealed how these promote an expansion of SOX2+ve stem cells in the embryonic and postnatal gland at the expense of differentiation. To establish if this effect was mediated through YAP alone, we used the tetracycline-controlled conditional YAP-TetO system to promote YAP (S127A) protein levels in postnatal pituitaries of $Hesx1^{Cre/+}$;$R26^{rtTA/+}$;$Col1a1^{tetO\text{-}Yap/+}$ mice. We treated YAP-TetO animals with doxycycline from P21 to P105 (12 week treatment, Fig5A). We did not observe the formation of tumours at any stage analysed (n=12, Figure 5 – figure supplement 1A). Similarly, we did not observe the formation of lesions when treating from P5. This is in contrast with the unequivocal tumour formation observed in $Sox2^{CreERT2/+}$;$Lats1^{fl/fl}$;$Lats2^{fl/+}$ mice. Elevation of YAP protein levels was confirmed following three weeks of doxycycline treatment (P42), displaying patchy accumulation, likely a result of genetic recombination efficiencies (Fig5B). Consistent with pathway activation, there was robust elevation in the expression of transcriptional targets *Cyr61* and *Ctgf* following treatment (Figure 5 –

figure supplement 1B), however at significantly lower levels compared to *Sox2*$^{CreERT2/+}$;*Lats1*$^{fl/fl}$;*Lats2*$^{fl/+}$ deletions (Figure 5 – figure supplement 1E), and there was no elevation in phosphorylated inactive YAP (Fig5B).

Immunofluorescence against SOX2 demonstrated a significant increase in the number of SOX2+ cells as a proportion of the anterior pituitary (Fig5B,F; 18.0% compared to 12.1% in controls, *P*=0.0014), a finding recapitulated by SOX9 that marks a subset of the SOX2 population (Fig5B). This increase in the percentage of SOX2+ cells was maintained at all stages analysed (Fig5F) and did not affect the overall morphology of the pituitary. At P42 we observed a significant increase in proliferation among the SOX2+ pituitary stem cells from 3% in controls to 15% in mutants (*P*=0.027). SOX2+ cells make up 10% of all cycling cells (Ki-67%) in normal pituitaries, however in mutants this increased to 25%, suggesting a preferential expansion of the SOX2+ population, rather than an overall increase in proliferation (Fig5C). No additional marked differences were observed in samples analysed at P63 (6 weeks of treatment, n=3), however longer treatment (P21 to P105) resulted in sporadic regions of expanded SOX2+ cells (Figure 5 – figure supplement 1C). These regions did not express the commitment marker PIT1 and were identifiable by haematoxylin/eosin staining. In contrast to tumour lesions generated following loss of LATS kinases, these were not proliferative, were positive for pYAP and did not accumulate high levels of YAP/TAZ (n=6 lesions). Together these results suggest that the sustained expression of constitutive active YAP can activate the proliferation of SOX2 stem cells, but in contrast to deletion of LATS1, this alone is not oncogenic.

To establish if the expansion of pituitary stem cells following forced expression of

YAP is reversible, we administered doxycycline to YAP-TetO animals for three weeks (P21 to P42) by which point there is a robust response, followed by doxycycline withdrawal for three weeks (until P63) to allow sufficient time for YAP levels to return to normal (scheme Fig5D). Immunofluorescence against total YAP protein confirmed restoration of the normal YAP expression pattern and levels after recovery (Fig5E), and mRNA *in situ* hybridisation detected a reduction in expression of YAP/TAZ targets *Cyr61* and *Ctgf* (Figure 5 – figure supplement 1D). Following recovery from high levels of YAP, the number of SOX2+ cells reduced to comparable levels as in controls (around 10% of the total anterior pituitary) (Fig5E,F). This suggests that the effects of YAP overexpression on the stem cell population are transient following three weeks of treatment (Fig5F).

Finally, to determine if SOX2+ cells could differentiate into hormone-producing cells after the reduction in YAP levels, we expressed constitutive active YAP only in SOX2+ cells whilst lineage tracing this population ($Sox2^{CreERT2/+};R26^{rtTA/mTmG};Col1a1^{tetO\text{-}Yap/+}$). We induced SOX2+ cells by low-dose tamoxifen administration at P21 and treated with doxycycline for three weeks, followed by doxycycline withdrawal for a further three weeks (Fig5G). Larger clones of SOX2 derivatives were observed at P63 in $Sox2^{CreERT2/+};R26^{rtTA/mTmG};Col1a1^{tetO\text{-}Yap/+}$ animals compared to controls, and these still contained SOX2+ cells (Fig5H). Following withdrawal, we were able to detect GFP+ derivatives of SOX2+ cells, which had differentiated into the three lineages (PIT1, SF1 and ACTH, marking corticotrophs of the TPIT lineage) (Fig5I). Taken together, these findings confirm that sustained expression of YAP is sufficient to maintain the SOX2+ state and promote activation of normal SOX2+ pituitary stem cells *in vivo*, driving expansion of this

population.

## DISCUSSION

Here we establish that regulation of LATS/YAP/TAZ signaling is essential during anterior pituitary development and can influence the activity of the stem/progenitor cell pool. LATS kinases, mediated by YAP and TAZ, are responsible for controlling organ growth, promoting an undifferentiated state and repressing lineage commitment. Loss of both *Lats1* and *Lats2*, encoding potent tumour suppressors, leads to dramatic tissue overgrowth during gestation, revealing a function for these enzymes in restricting growth during pituitary development. The involvement of YAP/TAZ and dysfunction of the kinase cascade is emerging in multiple paediatric cancers, which are often developmental disorders[37].

Loss of *LATS1* heterozygosity has been reported in a range of human tumours[38, 39, 40, 41] leading to an increase in YAP/TAZ protein levels. Previous global deletion of *Lats1* in mice resulted in a variety of soft tissue sarcomas and stromal cell tumours[42]. The anterior lobe of these animals appeared hyperplastic with poor endocrine cell differentiation leading to combined hormone deficiencies, but the presence of tumours was not noted. We report that loss of *Lats1* alone is sufficient to drive anterior and intermediate lobe tumour formation. This phenotype is accelerated following additional deletion of one copy of *Lats2*. Phenotypically identical tumour lesions were generated when the genetic deletions were carried out embryonically in RP, or at postnatal stages. Interestingly, tissue-specific loss of *Stk3* and *Stk4*, which regulate

LATS activation in other tissues[43], did not lead to any pituitary defects despite reduction in STK3/4 levels. These data suggest that perhaps the residual activity of STK3/4 is sufficient for LATS1/2 activation. Alternatively, regulation of LATS1/2 by kinases other than STK3/4 is possible in the pituitary, meaning deletion of *Stk3/4* alone is insufficient to result in significant LATS function impairment. Similar situations have been reported in other organs where LATS are functioning[43]. The resulting non-secreting tumours in our mouse models are composed predominantly of SOX2+ stem cells and display signs of squamous differentiation. Rare cases of squamous cell carcinoma have been reported as primary pituitary tumours[44], but more frequently, arising within cysts that are normally non-neoplastic epithelial malformations[45, 46]. In the embryonic YAP-TetO model, where constitutive active YAP (S127A) was expressed during pituitary development, cysts phenocopying Rathke's cleft cyst, develop by postnatal stages. Target elevation is not as high in YAP-TetO pituitaries, as following the deletion of LATS1/2, indicating that signaling levels are likely to be critical for progression between these phenotypes.

Although human pituitary carcinomas are only diagnosed as such after metastasis, the tumours generated in our LATS1/2 mouse models fit their histopathological profile. Genetic lineage tracing identified SOX2+ cells as the cell of origin of the tumours; this observation could have ramifications regarding involvement of the LATS/YAP/TAZ pathway in the establishment or progression of human pituitary tumours composed of uncommitted cells. In cancer stem cells of osteosarcoma and glioblastoma, SOX2 antagonises upstream Hippo activators, leading to enhanced YAP function[47]. We recently reported enhanced expression of YAP/TAZ in a range of non-functioning human pituitary tumours, compared to functioning adenomas, and that *Lats1* knock-down in GH3 pituitary mammosomatotropinoma cells results in

repression of the *Gh* and *Prl* promoters[28]. Therefore, YAP/TAZ, perhaps in a positive feedback loop with SOX2, are likely to function both to promote the maintenance of an active pituitary stem cell state as well as to inhibit differentiation.

By dissecting the downstream requirement for YAP in pituitary regulation by the LATS/YAP/TAZ axis, we found that expression of constitutively active YAP (S127A) is sufficient to push SOX2+ pituitary stem cells into an activated state, leading to expansion of the stem cell cohort (see Model, Fig6). YAP has previously been indicated to promote the stem cell state in other tissues, e.g. pancreas, neurons, mammary glands[48]. However, this does not fully recapitulate the LATS deletion phenotypes, as it did not lead to the formation of tumours during the time course of YAP activation (12 weeks). Interestingly, since the levels of target activation are significantly greater in *Lats1/2* deletions that in YAP-TetO activation, initiation of tumourigenesis may be associated with levels of signalling rising above a threshold. However, the temporal control of expressing the mutation is critical, as seen in other tumour models[49]. Instead, the findings identify an isolated role for YAP in promoting the expansion of the SOX2+ stem cell pool and restoring their proliferative potential to levels akin to the most active state during postnatal pituitary growth. Activity of YAP/TAZ is reduced in dense tissues, resulting in a decrease in stemness. One mechanism through which this is achieved is by crosstalk with other signaling pathways regulating stem cell fate[50, 51]. For example, a decrease in YAP/TAZ activity removes inhibition on Notch signalling, resulting in higher levels of differentiation and a drop in stem cell potential[52]. In the pituitary, Notch plays a role in the maintenance of the SOX2 stem cell compartment and is involved in regulating differentiation[53, 54, 55, 56]. The downstream mechanisms of YAP action on SOX2+

pituitary stem cells, as well as the likely crosstalk with other signalling pathways remain to be explored.

In summary, our findings highlight roles for LATS/YAP/TAZ in the regulation of pituitary stem cells, where fine-tuning of their expression can make the difference between physiological stem cell re-activation and tumourigenesis, of relevance to other organs. We reveal this axis is involved in the control of cell fate commitment, regulation of regenerative potential and promotion of tumourigenesis. These findings can aid in the design of treatments against pituitary tumours and in regenerative medicine approaches targeting the regulation of endogenous stem cells.

**ACKNOWLEDGEMENTS**

This study has been supported by grant MR/L016729/1 from the MRC and a Lister Institute Research Prize to C.L.A., by the Deutsche Forschungsgemeinschaft (DFG) within the CRC/Transregio 205/1 as well as GRK 2251 to C.L.A. and S.R.B. E.J.L. was supported by the King's Bioscience Institute and the Guy's and St Thomas' Charity Prize PhD Programme in Biomedical and Translational Science. J.P.R. was supported by a Dianna Trebble Endowment Fund Dental Institute Studentship. We thank Prof. Jacques Drouin and Prof. Simon Rhodes for TPIT and PIT1 antibodies respectively, and the National Hormone and Peptide Program (Harbor–University of California, Los Angeles Medical Center) for providing some of the hormone antibodies used in this study. We thank Prof. Juan Pedro Martinez-Barbera, Dr Rocio Sancho and Dr Marika Charalambous for discussions and critical reading of the manuscript. The authors declare no conflict of interest.

528

529 **MATERIALS & METHODS**

530 **Key Resources Table**

| Reagent type (species) or resource | Designation | Source or reference | Identifiers | Additional Information |
|---|---|---|---|---|
| Genetic reagent (*M. musculus*) | *Hesx1*$^{Cre/+}$ | PMID: 17360769 | RRID:MGI:5314529 | |
| Genetic reagent (*M. musculus*) | *Sox2*$^{CreERT2/+}$ | PMID: 24094324 | MGI:5512893 | |
| Genetic reagent (*M. musculus*) | *Lats1*$^{fl/fl}$ | Jackson Laboratory | Stock #: 024941, RRID: MGI:5568576 | |
| Genetic reagent (*M. musculus*) | *Lats2*$^{fl/fl}$ | Jackson Laboratory | Stock #: 025428, RRID: MGI:5568577 | |
| Genetic reagent (*M. musculus*) | *Stk4*$^{fl/fl}$;*Stk3*$^{fl/fl}$ | Jackson Laboratory | Stock #: 017635, RRID: MGI:5301573 | PMID: 20080689 |
| Genetic reagent (*M. musculus*) | R26$^{rtTA/+}$ | Jackson Laboratory | Stock: #: 016999 RRID: MGI:5292520 | PMID: 15941831 |
| Genetic reagent (*M. musculus*) | *Col1a1*$^{tetO\text{-}Yap/+}$ | PMID: 22363786 | MGI:5430522 | |
| Genetic reagent (*M. musculus*) | *R26*$^{mTmG/+}$ | Jackson Laboratory | Stock #: 007576 RRID:MGI:3722405 | PMID: 17868096 |
| Genetic reagent | *Taz*$^{-/-}$ | Jackson | Stock #: 011120, | PMID: |

| | | | | |
|---|---|---|---|---|
| (*M. musculus*) | | Laboratory | RRID: MGI:4420900 | 17636028 |
| Genetic reagent (*M. musculus*) | *Yap*$^{fl/fl}$ | PMID: 21376238 | MGI:5316446 | |
| Antibody | Rabbit polyclonal anti-TAZ | Atlas Antibodies | Cat# HPA007415 RRID:AB_1080602 | IF: 1:1000 |
| Antibody | Rabbit polyclonal anti-YAP | Cell Signaling Technology | Cat# 4912S RRID:AB_2218911 | IF: 1:1000 |
| Antibody | Rabbit polyclonal anti-pYAP | Cell Signaling Technology | Cat# 4911S RRID:AB_2218913 | IF: 1:1000 |
| Antibody | Rabbit polyclonal anti-SOX2 | Abcam | Cat# ab97959 RRID:AB_2341193 | IF: 1:2000 |
| Antibody | Rat monoclonal anti-EMCN (V.7C7.1) | Abcam | Cat# ab106100 RRID:AB_10859306 | IF: 1:1000 |
| Antibody | Chicken polyclonal anti-GFP | Abcam | Cat# ab13970 RRID:AB_300798 | IF: 1:300 |
| Antibody | Goat polyclonal anti-SOX2 | Immune Systems Limited | Cat# GT15098 RRID:AB_2732043 | IF: 1:250 |
| Antibody | Rabbit | Abcam | Cat# ab16667 | IF: 1:300 |

| | | | | |
|---|---|---|---|---|
| | monoclonal anti-Ki-67 | | RRID:AB_302459 | |
| Antibody | Rabbit polyclonal anti-ARL13B | Proteintech Group | Cat# 17711-1-AP, RRID:AB_2060867 | IF: 1:100 |
| Antibody | Mouse monoclonal anti-Acetylated-αTUB | Sigma-Aldrich | Cat# MABT868 | IF: 1:200 |
| Antibody | Rabbit monoclonal anti-SOX9 | Abcam | Cat# ab185230 RRID:AB_2715497 | IF: 1:300 |
| Antibody | Rabbit monoclonal anti-Active YAP EPR19812 | Abcam | Cat# ab205270 | IF: 1:300 |
| Antibody | Rabbit polyclonal anti-PIT1 | Prof. S. Rhodes (Indiana University | | IF: 1:1000 |
| Antibody | Rabbit polyclonal anti-TPIT | Prof. J. Drouin (Montreal IRCM) | | IF: 1:1000 |
| Antibody | Mouse monoclonal | Life Technologies | Cat# N1665 RRID:AB_2532209 | IF: 1:200 |

| | | | | |
|---|---|---|---|---|
| | anti-SF1 | (Thermo Fisher Scientific) | | |
| Antibody | Rabbit polyclonal anti-gamma H2A.X (phospho S139) | Abcam | Cat# ab2893 RRID:AB_303388 | IF: 1:1000 |
| Antibody | Rabbit polyclonal anti-STK3/4 | Bethyl Laboratories | Cat# A300-466A RRID:AB_2148394 | WB: 1:5000 |
| Antibody | Mouse monoclonal anti-Cyclophilin B (Clone# 549205) | R&D Systems | Cat# MAB5410 RRID:AB_2169416 | WB: 1:1000 |
| Antibody | Rabbit monoclonal anti-Vimentin (D21H3) | Cell Signaling Technology | Cat# 5741 RRID:AB_10695459 | IF: 1:300 |
| Antibody | Biotinylated Goat polyclonal anti-rabbit | Abcam | Cat# ab6720 RRID:AB_954902 | IF: 1:350 |
| Antibody | Goat polyclonal anti-chicken | Life Technologies | Cat# A11039 RRID:AB_2534096 | IF: 1:300 |

| | | | | |
|---|---|---|---|---|
| | Alexa Fluor 488 | (Thermo Fisher Scientific) | | |
| Antibody | Goat polyclonal anti-rat Alexa Fluor 555 | Life Technologies (Thermo Fisher Scientific) | Cat# A21434 RRID:AB_2535855 | IF: 1:300 |
| Antibody | Biotinylated Goat polyclonal anti-mouse | Abcam | Cat# ab6788 RRID:AB_954885 | IF: 1:350 |
| Antibody | Donkey polyclonal anti-goat Alexa Fluor 488 | Abcam | Cat# ab150133 | IF: 1:300 |
| Antibody | Streptavidin Alexa Fluor 555 | Life Technologies | Cat# S21381 RRID:AB_2307336 | IF: 1:500 |
| Antibody | Goat HRP-linked anti-rabbit | Cell Signaling Technology | Cat# 7074 RRID:AB_2099233 | WB: 1:2000 |
| Antibody | Goat HRP-linked anti-mouse | Cell Signaling Technology | Cat# 7076 RRID:AB_330924 | WB: 1:2000 |
| Antibody | Mouse monoclonal | Dako | Cat# M351529 | IHC: 1:100 |

| | | | | |
|---|---|---|---|---|
| | anti-AE1/AE3 | | | |
| Antibody | Mouse monoclonal anti-Chromogranin | Dako | Cat# M086901 | IHC: 1:400 |
| Antibody | Mouse monoclonal anti-NCAM | Novocastra | Cat# NCL-L-CD56-504 | IHC 1:15 |
| Antibody | Mouse monoclonal anti-NSE | Dako | Cat# M087329 | IHC 1:1000 |
| Antibody | Mouse monoclonal anti-p63 | A. Menarini Diagnostics | Cat# MP163 | IHC 1:100 |
| Antibody | Mouse monoclonal anti-Synaptophysin | Dako | Cat# M731529 RRID:AB_2687942 | IHC 1:2 |
| Commercial assay or kit | TSA kit | Perkin Elmer | Cat# NEL753001KT | |
| Commercial assay or kit | TSA Blocking Reagent | Perkin Elmer | Cat# FP1020 | |
| Commercial assay or kit | ABC kit | Vector Laboratories | Cat# Vector PK-6100 RRID:AB_2336819 | |
| Commercial | BCA assay | Thermo Fisher | Cat# 23227 | |

| | | | | |
|---|---|---|---|---|
| assay or kit | | | | |
| Commercial assay or kit | UltraView Universal DAB Detection Kit | Ventana Medical Systems | Cat# 760-500 | |
| Commercial assay or kit | VectaFluor Excel R.T.U. Antibody Kit, DyLight 488 Anti-Mouse | Vector Laboratories | Cat# DK-2488 RRID:AB_2336775 | |
| Chemical compound, drug | Doxycycline hyclate | Alfa Aesar | Cat# J60579 | 2mg/ml |
| Chemical compound, drug | Sucrose | Sigma-Aldrich | Cat# S0389 | 10mg/ml |
| Chemical compound, drug | Tamoxifen | Sigma-Aldrich | Cat# T5648 | 0.15mg/g |
| Chemical compound, drug | Hoechst 33342 | Life Technologies | Cat# H3570 | 1:10000 |
| Chemical compound, drug | Laemmli buffer | Bio-Rad | Cat# 1704156 | |
| Chemical compound, drug | Clarity Western ECL Substrate | Bio-Rad | Cat# 170-5060 | |
| Chemical compound, drug | Alcian Blue | Alfa Aeser | Cat# J60122 | 1% |
| Chemical compound, drug | Acetic acid | VWR | Cat# 20103 | 3% |

| | | | | |
|---|---|---|---|---|
| Chemical compound, drug | Periodic acid | VWR | Cat# 29460 | 1% |
| Chemical compound, drug | Schiff's reagent | Thermo Fisher Scientific | Cat# 88017 | |
| Software, algorithm | GraphPad Prism | GraphPad Software (www.graphpad.com) | RRID:SCR_015807 | |
| Software, algorithm | Fiji | Schindelin *et al*., 2012 (Fiji.sc) | RRID:SCR_002285 | |
| Software, algorithm | ImageLab | BioRad | | |
| Other | Probe: *Ctgf* | ACDBio | Cat# 314541 | |
| Other | Probe: *Cyr61* | ACDBio | Cat# 429001 | |
| Other | Probe: *Lats2* | ACDBio | Cat# 420271 | |
| Other | Probe: *Nr5a1* | ACDBio | Cat# 445731 | |
| Other | Probe: *Tbx19* | ACDBio | Cat# 484741 | |
| Other | Probe: *Pou1f1* | ACDBio | Cat# 486441 | |

**Animals**

Animal husbandry was carried out under compliance of the Animals (Scientific Procedures) Act 1986, Home Office license and KCL ethical review approval.

The *Hesx1*$^{Cre/+}$ [57], *Sox2*$^{CreERT2/+}$ [1], *Yap*$^{fl/fl}$ [25], *Taz*$^{-/-}$ [30](JAX:011120), *R26*$^{mTmG/+}$ [58](JAX:007576), *ROSA26*$^{rtTA/+}$ [59] (JAX:016999), *Col1a1*$^{tetO\text{-}Yap/+}$ [60](MGI:5430522), *Stk3*$^{fl/fl}$;*Stk4*$^{fl/fl}$ [61](JAX:017635), and *Lats1*$^{fl/fl}$ [51](JAX:024941) and *Lats2*$^{fl/fl}$ [51](JAX:025428) have been previously described.

Tamoxifen (Sigma, T5648) was administered to experimental mice by intraperitoneal injection at a single dose of 0.15mg/g body weight, or two equal doses on sequential days, depending on the experiment. Mice for growth studies were weighed every week. For embryonic studies, timed matings were set up where noon of the day of vaginal plug was designated as 0.5dpc.

For YAP-TetO experiments, crosses between *Hesx1*$^{Cre/+}$;*R26*$^{+/+}$;*Col1a1*$^{+/+}$ and *Hesx1*$^{+/+}$;*R26*$^{rtTA/rtTA}$;*Col1a1*$^{tetO\text{-}Yap/\ tetO\text{-}Yap}$ animals were set up to generate *Hesx1*$^{Cre/+}$;*R26*$^{rtTA/+}$;*Col1a1*$^{tetO\text{-}Yap/+}$ offspring (hereby YAP-TetO) and control littermates, or crosses between *Sox2*$^{CreERT2/+}$;*R26*$^{mTmG/mTmG}$;*Col1a1*$^{+/+}$ and *Sox2*$^{+/+}$; *R26*$^{rtTA/rtTA}$;*Col1a1*$^{tetO\text{-}Yap/\ tetO\text{-}Yap}$ animals were set up to generate *Sox2*$^{CreERT2/+}$;*R26*$^{rtTA/mTmG}$;*Col1a1*$^{tetO\text{-}Yap/+}$ offspring. Whilst treated with the tetracycline analogue doxycycline, YAP-TetO expressed rtTA from the *ROSA26* locus in *Cre*-derived cells, enabling YAP S127A expression from the *Col1a1* locus. For embryonic studies between 5.5dpc and 15.5dpc (scheme, Fig1A), doxycycline (Alfa Aesar, J60579) was administered to pregnant dams in the drinking water at 2mg/ml, supplemented with 10% sucrose. For postnatal analyses animals were treated with doxycycline or vehicle (DMSO) as described, from the ages specified for individual experiments on the *Hesx1*$^{Cre/+}$ driver, or directly following tamoxifen administration for animals on the *Sox2*$^{CreERT2/+}$ driver. Both male and female mice and embryos where included in the studies.

**Tissue preparation**

Embryos and adult pituitaries were fixed in 10% neutral buffered formalin (Sigma) overnight at room temperature. The next day, tissue was washed then dehydrated through graded ethanol series and paraffin-embedded. Embryos up to 13.5dpc were sectioned sagittal and all older embryo and postnatal samples were sectioned frontal, at a thickness of 7µm for immunofluorescence staining, or 4µm for RNAscope mRNA *in situ* hybridisation.

**RNAscope mRNA *in situ* hybridisation**

Sections were selected for the appropriate axial level, to include Rathke's pouch or pituitary, as described previously [27]. The RNAscope 2.5 HD Reagent Kit-RED assay (Advanced Cell Diagnostics) was used with specific probes: *Ctgf, Cyr61, Lats2* (all ACDBio).

**H&E staining**

Sections were dewaxed in histoclear and rehydrated through graded ethanol series from 100% to 25% ethanol, then washed in distilled $H_2O$. Sections were stained with Haematoxylin QS (Vector #H3404) for 1 minute, and then washed in water. Slides were then stained in eosin in 70% ethanol for 2 minutes and washed in water. Slides were dried and coverslips were mounted with VectaMount permanent mounting medium (Vector Laboratories H5000).

**Immunofluorescence and immunohistochemistry**

Slides were deparaffinised in histoclear and rehydrated through a descending graded ethanol series. Antigen retrieval was performed in citrate retrieval buffer pH6.0, using

a Decloaking Chamber NXGEN (Menarini Diagnostics) at 110°C for 3mins. Tyramide Signal Amplification (TSA) was used for staining using antibodies against YAP (1:1000, Cell Signaling #4912S), pYAP (1:1000, Cell Signaling #4911S), TAZ (1:1000, Atlas Antibodies #HPA007415) and SOX2 (1:2000, Abcam ab97959) with EMCN (1:1000, Abcam ab106100) staining as follows: sections were blocked in TNB (0.1M Tris-HCl, pH7.5, 0.15M NaCl, 0.5% Blocking Reagent (Perkin Elmer FP1020)) for 1 hour at room temperature, followed by incubation with primary antibody at 4C overnight, made up in TNB. Slides were washed three times in TNT (0.1MTris-HCl pH7.5, 0.15M NaCl, 0.05% Tween-20) then incubated with secondary antibodies (biotinylated anti-rabbit (1:350 Abcam ab6720) and anti-Rat Alexa Fluor 555 (1:300, Life Technologies A21434) for 1 hour at room temperature and Hoechst (1:10000, Life Technologies H3570). Slides were washed again then incubated in ABC reagent (ABC kit, Vector Laboratories PK-6100) for 30 mins, followed by incubation with TSA conjugated fluorophore (Perkin Elmer NEL753001KT) for ten minutes. Slides were washed and mounted with VectaMount (Vector Laboratories H1000).

For regular immunofluorescence sections were blocked in blocking buffer (0.15% glycine, 2mg/ml BSA, 0.1% Triton-X in PBS), with 10% sheep serum (donkey serum for goat SOX2 antibody) for 1 hour at room temperature, followed by incubation with primary antibody at 4C overnight, made up in blocking buffer with 1% serum. Primary antibodies used were against SOX2 (1:250, Immune Systems Ltd GT15098), active YAP (1:300, Abcam ab205270), GFP (1:300, Abcam ab13970), Ki-67 (1:300, Abcam ab16667), SOX9 (1:300, Abcam ab185230), PIT1 (1:1000, Gift from S. Rhodes, Indiana University), TPIT (1:1000, Gift from J. Drouin, Montreal), SF1 (1:200, Life Technologies N1665), Gamma H2A.X (1:1000, Abcam ab2893),

Vimentin (1:300, Cell Signaling #5741), Caspase (1:300, Cell Signaling #9661S). Slides were washed in PBST then incubated with secondary antibodies for 1 hour at room temperature. Appropriate secondary antibodies were incubated in blocking buffer for 1 hr at room temperature (biotinylated anti-rabbit (1:350, Abcam ab6720), biotinylated anti-mouse (1:350, Abcam ab6788), anti-chicken 488 (1:300, Life Technologies A11039), anti-goat 488 (1:300, Abcam ab150133). Slides were washed again using PBST and incubated with fluorophore-conjugated Streptavidin (1:500, Life Technologies S21381 or S11223) for 1 hour at room temperature, together with Hoechst (1:10000, Life Technologies H3570). Slides were washed in PBST and mounted with VectaMount (Vector Laboratories, H1000).

Immunohistochemistry for the remaining antigens were undertaken on a Ventana Benchmark Autostainer (Ventana Medical Systems) using the following primary antibodies and antigen retrieval: AE1/AE3 (1:100, Dako M351529), CC1 (36 minutes, Ventana Medical Systems 950-124); Chromogranin (1:400, Dako M086901), CC1 (36 minutes, Ventana Medical Systems 950-124); NCAM (1:15, Novocastra NCL-L-CD56-504), CC1 (64 minutes, Ventana Medical Systems 950-124); NSE (1:1000, Dako M087329), CC1 (36 minutes, Ventana Medical Systems 950-124); p63 (1:100, A. Menarini Diagnostics), CC1 (64 minutes, Ventana Medical Systems 950-124) and Synaptophysin (1:2, Dako M731529), CC2 (92 minutes, Ventana Medical Systems 950-124). Targets were detected and viewed using the ultraView Universal DAB Detection Kit (Ventana Medical Systems, 760-500) according to manufacturer's instructions.

**Alcian Blue with Periodic Acid-Schiff staining (AB/PAS)**

Following deparaffinisation and rehydration, sections were taken through distilled water then placed in Alcian Blue solution (1% Alcian Blue (Alfa Aeser J60122) in 3% acetic acid (VWR International 20103)) for 20 minutes. Sections were then placed in 1% periodic acid (VWR 29460) for 10 minutes, washed in distilled water and transferred to Schiff's reagent (Thermo Fisher Scientific 88017) for 10 minutes, followed by washing in distilled water for 5 minutes. Sections were then routinely dried, cleared and mounted.

**Western blotting**

Dissected anterior pituitaries were flash frozen in liquid nitrogen and stored at -80°C. Frozen pituitaries were each lysed in 30µl of lysis buffer (5mM Tris, 150mM NaCl, 1% protease and phosphatase inhibitor (Abcam ab201119), 5µM EDTA, 0.1% Triton-X, pH7.6) and sonicated at 40% power, twice for ten cycles of: two seconds on/two seconds off, using a Vibra-Cell Processor (Sonics). Protein concentration was determined using the Pierce BCA protein assay kit (Thermo #23227) and all samples were diluted to 4mg/ml in Laemmli buffer (Biorad #161-0747). Proteins were denatured at 95°C for 5 minutes. Samples were run on a 10% Mini-PROTEAN TGX polyacrylamide gel (BioRad #4561033), then transferred using Trans-Blot Turbo transfer machine (BioRad) onto polyvinylidene difluoride membranes (BioRad #1704156). Membranes were blocked with 5% non-fat dairy milk (NFDM) in TBST (20mM Tris, 150mM NaCl, 0.1% Tween-20, pH7.6), cut, then incubated with primary antibodies overnight at 4°C as follows: anti-STK3/STK4 (1:5000, Bethyl Laboratories #A300-466A) or Cyclophilin B (1:1000, R&D Systems #MAB5410) in 5%NFDM. The next day, membranes were washed in TBST, incubated with secondary antibodies HRP-conjugated anti-Rabbit (1:2000, Cell Signaling #7074) or

HRP-conjugated anti-Mouse (1:2000, Cell Signaling #7076) in 5% NFDM for 1hr at room temperature. After washing in TBST, membranes were treated with Clarity Western ECL substrate (Biorad #170-5060) and bands visualised using the ChemiDoc Touch Imaging System (BioRad). Protein abundance was analysed using ImageLabs (BioRad).

**Imaging**

Wholemount images were taken with a MZ10 F Stereomicroscope (Leica Microsystems), using a DFC3000 G camera (Leica Microsystems). For bright field images, stained slides were scanned with Nanozoomer-XR Digital slide scanner (Hamamatsu) and images processed using Nanozoomer Digital Pathology View. Fluorescent staining was imaged with a TCS SP5 confocal microscope (Leica Microsystems) and images processed using Fiji [62].

**Quantifications and Statistics**

Cell counts were performed manually using Fiji cell counter plug-in; 5-10 fields were counted per sample, totalling over 1500 nuclei, across 3-7 pituitaries. Statistical analyses and graphs were generated in GraphPad Prism (GraphPad Software) and the following tests were performed to determine significance: Student's *t*-tests between controls and mutants for Figures 1D, 2D, S1bD, S1bE (n=3 of each genotype), S4 (n=4 of each genotype) and 5C (n=4-5 of each genotype); unpaired *t*-test for Figures S2bA (n=3 per genotype) and S2bF (n=6 sections across two samples per genotype); two-tailed *t*-test for Figure 3C (n=3 controls, 7 mutants); two-way ANOVA with Sidak's multiple-comparison test for Figures 5F (n=4-5 of each genotype). For quantification of target expression by RNAscope mRNA *in situ* hybridisation (Figure

S5), the area of positive staining (red fluorescence) from 4μm sections was determined from images using thresholding in Fiji, and quantified as a percentage of total pituitary area in the same image. For statistical testing, one-way ANOVAs with Tukey's multiple comparisons were performed (n=4 mutants per genotype). Error bars in graphs show ± standard error of the mean, unless otherwise indicated. Quantification of STK3/4 by western blot was carried out on 2 control (*Stk3*$^{fl/fl}$;*Stk4*$^{fl/fl}$) and 3 mutant (*Hesx1*$^{Cre/+}$;*Stk3*$^{fl/fl}$; *Stk4*$^{fl/fl}$) samples. A Student's t-test was carried out on normalised band intensities. Chi-squared tests were used to determine significant deviations of observed from expected genotypes presented as tables in Supplementary Files 1 and 2.

## FIGURE LEGENDS

**Figure 1 Regulation of YAP is required for normal morphogenesis and lineage commitment during pituitary development.**

**A.** Schematic outlining the time course of doxycycline (DOX) treatment administered to pregnant dams from *Hesx1*$^{Cre/+}$ x *R26*$^{rtTA/rtTA}$;*Col1a1*$^{tetO\text{-}Yap/tetO\text{-}Yap}$ crosses for the embryonic induction of YAP(S127A) expression in *Hesx1*$^{Cre/+}$;*R26*$^{rtTA/+}$;*Col1a1*$^{tetO\text{-}Yap/+}$ (YAP-TetO) mutant embryos as well as controls that do not express YAP(S127A) (*Hesx1*$^{+/+}$;*R26*$^{rtTA/+}$;*Col1a1*$^{tetO\text{-}Yap/+}$ controls shown here). **B.** Immunofluorescence staining against YAP and TAZ on frontal pituitary sections at 15.5dpc confirms accumulation of YAP protein in YAP-TetO compared to control sections, but no increase in TAZ levels. RNAscope mRNA *in situ* hybridisation against the YAP/TAZ target *Cyr61* confirms an increase in transcripts in the anterior pituitary as well as the hypothalamus where the Cre is also active (arrows). **C.** Haematoxylin and eosin staining of frontal pituitary sections from 15.5dpc control and YAP-TetO embryos showing pituitary dysmorphology in mutants. Immunofluorescence staining for LHX3 to mark anterior pituitary tissue and SOX2 to mark pituitary progenitors shows the persistence of SOX2 protein in lateral regions of

the gland in YAP-TetO mutants (arrowheads) when they have lost SOX2 expression in controls (arrows) (magnified boxed region in SOX2, corresponding to dashed box in LHX3). **D.** Immunofluorescence staining for lineage-committed progenitor markers PIT1, TPIT and SF1 reveals very few cells expressing commitment markers in YAP-TetO compared to control. Graph showing quantification of committed cells of the three anterior pituitary endocrine lineages, positive for PIT1, TPIT and SF1, as a percentage of total nuclei of *Hesx1*$^{+/+}$;*R26*$^{rtTA/+}$;*Col1a1*$^{tetO\text{-}Yap/+}$ control and *Hesx1*$^{Cre/+}$;*R26*$^{rtTA/+}$;*Col1a1*$^{tetO\text{-}Yap/+}$ (YAP-TetO) mutant pituitaries at 15.5dpc (Student's *t*-test; PIT1: $P<0.0001$ (****), TPIT: $P=0.0012$ (**), SF1: $P=0.0021$ (**)). Scale bars 100μm, 50μm in magnified boxed regions in C. See also figure supplements 1 and 2.

**Figure 2 Pituitary-specific deletion of *Lats1* and *Lats2* during development leads to pituitary overgrowth and defects in lineage commitment.**

**A.** Haematoxylin and eosin staining on sagittal sections from *Hesx1*$^{Cre/+}$;*Lats1*$^{fl/fl}$;*Lats2*$^{fl/fl}$ (mutant) and *Hesx1*$^{+/+}$;*Lats1*$^{fl/fl}$;*Lats2*$^{fl/fl}$ (control) embryos at 13.5dpc reveals anterior pituitary dysmorphology and overgrowth in mutants (dashed outline). Immunofluorescence staining for TAZ, YAP and pYAP reveals accumulation of TAZ and YAP in overgrown mutant tissue (arrowheads, normal epithelial expression indicated by arrows in control) and lack of staining for pYAP (S127). Immunofluorescence for SOX2 shows the presence of SOX2+ progenitors throughout the abnormal tissue in mutants. **B.** Immunofluorescence staining for late progenitor marker SOX9 shows localisation in few cells of the pituitary of mutants at 13.5dpc. Immunofluorescence staining for Ki-67 indicates cycling cells throughout the mutant pituitary. **C.** Immunofluorescence staining for SOX2 and Endomucin (EMCN) on frontal pituitary sections at 15.5dpc shows expansion of the SOX2+ progenitor compartment compared to controls and a reduction in vasculature marked by Endomucin. Immunofluorescence for non-phosphorylated (Active) YAP shows strong expression throughout the mutant gland compared to the control. Areas of necrosis in mutant tissue indicated by asterisks. Ventral overgrowth extending into the oral cavity between the condensing sphenoid bone indicated by arrows. **D.** Immunofluorescence staining for lineage-committed progenitor markers PIT1, TPIT and SF1 reveals only sporadic cells expressing

commitment markers in *Hesx1*$^{Cre/+}$;*Lats1*$^{fl/fl}$;*Lats2*$^{fl/fl}$ mutants compared to controls. Boxes showing magnified regions. Dashed lines demarcate anterior pituitary tissue. Graph showing quantification of committed cells of the three anterior pituitary endocrine lineages, positive for PIT1, TPIT and SF1, as a percentage of total nuclei of *Hesx1*$^{+/+}$;*Lats1*$^{fl/fl}$;*Lats2*$^{fl/fl}$ control and *Hesx1*$^{Cre/+}$;*Lats1*$^{fl/fl}$;*Lats2*$^{fl/fl}$ mutant pituitaries at 15.5dpc (Student's *t*-test; PIT1: $P<0.0001$ (****), TPIT: $P=0.007$ (**), SF1: $P>0.05$). Scale bars 100μm. See also figure supplement 2.

**Figure 3 Pituitary specific loss of *Lats1* leads to tumour formation.**

**A.** Haematoxylin and eosin staining of frontal sections from *Hesx1*$^{Cre/+}$;*Lats1*$^{fl/fl}$;*Lats2*$^{fl/+}$ (mutant) and control pituitaries at P56 demonstrates overgrown tumourigenic regions in mutants. These show focal necrosis, cysts and a squamous morphology (magnified regions) not seen in controls. Asterisk indicates necrosis. **B.** Immunofluorescence staining for TAZ, YAP and pYAP(S127) show accumulation of TAZ and YAP but not pYAP in the mutant but not in the control. RNAscope mRNA *in situ* hybridisation against YAP/TAZ targets *Ctgf* and *Cyr61* reveals an increase in transcripts on mutant tissue compared to control. **C.** Graph of the proliferation index in control and mutant samples at P56 shows a significant increase in cycling cells in the *Hesx1*$^{Cre/+}$;*Lats1*$^{fl/fl}$;*Lats2*$^{fl/+}$ mutant pituitaries compared to controls (control percentage Ki-67: 2.967±1.2 SEM, n=3; mutant: 15.46±2.74 n=7. $P=0.0217$ (*), two-tailed *t*-test). Images show representative examples of Ki-67 immunofluorescence staining. **D.** Immunofluorescence staining for lineage-committed progenitor markers PIT1, TPIT and SF1 shows the near absence of committed cells in tumours. **E.** Immunofluorescence staining for pituitary stem cell markers SOX2 and SOX9 reveal that tumour lesions have abundant positive cells compared to the control, whilst Endomucin (EMCN) staining shows poor vascularisation. **F.** The marginal zone epithelium of *Hesx1*$^{Cre/+}$;*Lats1*$^{fl/fl}$;*Lats2*$^{fl/+}$ mutant pituitaries develops invaginations as seen by haematoxylin and eosin staining. Immunofluorescence staining against SOX2 shows the maintenance of a single-layered epithelium. Scale bars 100 μm. Boxes indicate magnified regions. See also figure supplement 1.

**Figure 4 SOX2+ pituitary stem cells are the cell-of-origin of tumours generated in the absence of *Lats1*.**

**A.** Schematic outlining the experimental time line of inductions in *Sox2*$^{CreERT2/+}$;*Lats1*$^{fl/fl}$;*Lats2*$^{fl/+}$ (mutant) and *Sox2*$^{+/+}$;*Lats1*$^{fl/fl}$;*Lats2*$^{fl/+}$ (control) animals. Representative images of haematoxylin and eosin staining of frontal sections of control and mutant pituitaries at P35, revealing a hyperplastic anterior pituitary in the mutant with areas of necrosis (asterisks). **B.** Immunofluorescence staining reveals tumourigenic lesions in *Sox2*$^{CreERT2/+}$;*Lats1*$^{fl/fl}$;*Lats2*$^{fl/+}$ that display increased levels of TAZ and YAP staining compared to the control. **C.** RNAscope mRNA *in situ* hybridisation against *Ctgf* and *Cyr61* shows elevated transcripts in tumourigenic lesions. Insets (i) and (ii) show invaginations in the epithelium of the mutant. **D.** Immunofluorescence staining for lineage-committed progenitor markers PIT1, TPIT and SF1 showing a reduction in staining in tumourigenic lesions compared to control pituitaries. **E.** Lineage tracing of SOX2+ cells in *Sox2*$^{CreERT2/+}$;*Lats1*$^{fl/fl}$;*Lats2*$^{fl/+}$*R26*$^{mTmG/+}$ reveals that tumour regions accumulating YAP as seen by immunofluorescence, are composed of GFP+ cells at P35. Scale bars 500µm in A; 100µm in B, D, E; 250µm in C. See also figure supplement 1.

**Figure 5 Postnatal expression of constitutively active YAP increases leads to an activation of SOX2+ pituitary stem cells.**

**A.** Schematic outlining the time course of doxycycline (DOX) treatment administered to *Hesx1*$^{Cre/+}$;*R26*$^{rtTA/+}$;*Col1a1*$^{tetO\text{-}Yap/+}$ (YAP-TetO) and *Hesx1*$^{+/+}$;*R26*$^{rtTA/+}$;*Col1a1*$^{tetO\text{-}Yap/+}$ controls to drive expression of YAP-S127A in mutant pituitaries. **B.** At P42 (3 weeks of treatment), immunofluorescence staining on frontal anterior pituitary sections detects strong total YAP expression in YAP-TetO mutants compared to the control and no increase in pYAP(S127). Immunofluorescence for SOX2 and SOX9 reveals an expanded population of stem cells in YAP-TetO compared to control (quantification in F). **C.** Graph showing the percentage of double Ki-67+SOX2+ cells as a proportion of the total SOX2+ ($P$=0.027 (*)) or Ki-67+ ($P$=0.006 (**)) populations at P42 (n=3 pituitaries per genotype). There is an increase in the numbers of cycling SOX2 cells in YAP-TetO mutant compared to controls. The image shows a representative example of double immunofluorescence staining against Ki-67 and SOX2 in a control and YAP-TetO section. **D.** Schematic outlining the time course of doxycycline (DOX) treatment administered to *Hesx1*$^{Cre/+}$;*R26*$^{rtTA/+}$;*Col1a1*$^{tetO\text{-}Yap/+}$ (YAP-TetO) and *Hesx1*$^{+/+}$;*R26*$^{rtTA/+}$;*Col1a1*$^{tetO\text{-}Yap/+}$ controls to drive expression of YAP-S127A in mutant pituitaries for three weeks, followed by a three-week recovery

period in the absence of DOX. **E.** Immunofluorescence staining against YAP, SOX2 and SOX9 on control and YAP-TetO pituitaries treated as in D, shows comparable expression of YAP, SOX2 and SOX9 between genotypes. **F.** Graph of quantification of SOX2+ cells as a percentage of total nuclei in control and YAP-TetO pituitaries at P42 $P$=0.0014 (**); P63 $P$=0.0044 (**); P105 $P$<0.0001(****) (n=3 pituitaries per genotype). Following the Recovery treatment scheme in D, there is no significant difference in the numbers of SOX2+ cells between genotypes. **G.** Schematic outlining the time course of tamoxifen induction and doxycycline (DOX) treatment administered to $Sox2^{CreERT2/+};R26^{rtTA/mTmG};Col1a1^{tetO\text{-}Yap/+}$ (mutant) and $Sox2^{CreERT2/+};R26^{mTmG/+};Col1a1^{+/+}$ (control) animals to drive expression of YAP-S127A in SOX2+ cells of mutants. **H.** Lineage tracing of SOX2+ cells and immunofluorescence staining against SOX2 and GFP shows an expansion of GFP+ cells compared to controls at P63, where a proportion of cells are double-labelled. **I.** Immunofluorescence staining against commitment markers PIT1, SF1 and terminal differentiation marker ACTH (TPIT lineage) together with antibodies against GFP detects double-labelled cells (arrows) across all three lineages in $Sox2^{CreERT2/+};R26^{rtTA/mTmG};Col1a1^{tetO\text{-}Yap/+}$ pituitaries following the recovery period. Graph of quantification of GFP+;PIT1+, GFP+;SF1+ and GFP+;ACTH+ cells as a percentage of total GFP+ cells in $Sox2^{CreERT2/+};R26^{rtTA/mTmG};Col1a1^{tetO\text{-}Yap/+}$ pituitaries at P63. Scale bars 100μm. Data in C. and F. represented as mean ± SEM, analysed with Two-Way ANOVA with Sidak's multiple comparisons. See also figure supplement 1.

**Figure 6 Model of stem cell activity following regulation by the LATS/YAP/TAZ cascade in the anterior pituitary.**

SOX2+ pituitary stem cells express YAP and TAZ (green spheres). During normal developmental and postnatal expansion (normal regulation), pituitary stem cells are maintained as a balanced pool while generating endocrine cells of three committed lineages (red, blue, yellow). Expression of constitutively active YAP-S127A in pituitary stem cells leads to an elevation in target gene expression, an expansion of pituitary stem cell numbers and maintenance of the SOX+ state, preventing lineage commitment. When YAP-S127A expression ceases, commitment into the endocrine lineages takes place. Genetic deletion of LATS kinases (LATS1 as well as one or two copies of LATS2), results in YAP and TAZ accumulation, major elevation in target

gene expression, repression of lineage commitment, continued expansion of SOX2+ cells and tumour formation.

## FIGURE SUPPLEMENT LEGENDS

**Figure 1 – figure supplement 1 Regulation of YAP and TAZ during pituitary development.**

**A.** Hematoxylin and eosin staining on frontal sections through the pituitary from control and YAP-TetO heads after DOX treatment from 5.5dpc until 15.5dpc. **B.** Schematic outlining the time course of doxycycline (DOX) treatment administered to *Hesx1*$^{Cre/+}$;*R26*$^{rtTA/+}$;*Col1a1*$^{tetO\text{-}Yap/+}$ (YAP-TetO) and *Hesx1*$^{+/+}$;*R26*$^{rtTA/+}$;*Col1a1*$^{tetO\text{-}Yap/+}$ controls to drive expression of YAP-S127A in mutant pituitaries during embryonic as well as postnatal development. **C.** Hematoxylin and eosin (H&E) staining of control and YAP-TetO pituitaries at P24. Higher magnification images show the presence of cysts in the YAP-TetO mutant. White arrows indicate cells with enlarged nuclei surrounding the cysts and yellow arrows indicate ciliated cells. **D.** Immunofluorescence staining against total YAP on frontal sections at P24 confirms accumulation of YAP protein in YAP-TetO compared to control sections, especially in the ventral anterior lobe. Immunofluorescence staining against SOX2 shows an expansion of SOX2+ epithelia lining cysts. **E.** Immunofluorescence staining for lineage-committed progenitor markers PIT1, TPIT and of ACTH marking the SF1 lineage in control and YAP-TetO sections at P24. The number of SOX2+ and lineage-committed cells is quantified in the graph below. Note there is a significant increase in the proportion of SOX2+ cells in YAP-TetO mutants (Student's *t*-test, $P<0.0001$ (****)), decrease in PIT1+ cells (Student's *t*-test, $P<0.0002$ (***)), increase in SF1+ cells (Student's *t*-test, $P<0.0066$ (**)) and no significant change in ACTH+ cells. **F.** Immunofluorescence staining against Ki-67 marking cycling cells in control and YAP-TetO sections at P24. Graph showing the percentage of Ki-67+ cells across total anterior pituitary cells. There is a trend towards a reduction in the proportion of cycling cells in YAP-TetO mutants, which is not significant (Student's *t*-test, $P>0.05$). **G.** Immunohistochemistry using antibodies against p63 and the AE1/AE3 cytokeratin cocktail in YAP-TetO mutants at P24 revealing positive cells lining the

cysts (arrowheads). **H.** Immunofluorescence staining using antibodies against ARL13B and Acetylated α-Tubulin, staining components of cilia, reveals ciliated cells lining the cysts. Staining for Alcian Blue and Period Acid Schiff (AB/PAS) to differentiate between acidic and neutral mucins reveals royal blue-stained mucous cells lining the cysts. Scale bars 1mm in A, 500µm in C and 100µm in magnified panels in C, 100µm in D, E, F and 50µm in G and H.

**Figure 1 – figure supplement 2 Regulation of YAP and TAZ during pituitary development.**

**A.** Hematoxylin and eosin staining on sagittal pituitary sections of 13.5dpc *Hesx1*$^{Cre/+}$;*Yap*$^{fl/fl}$;*Taz*$^{-/-}$ (mutant) and *Hesx1*$^{+/+}$;*Yap*$^{fl/+}$;*Taz*$^{+/-}$ (control) showing comparable morphology. **B.** Immunofluorescence staining using antibodies against SOX2 in *Hesx1*$^{Cre/+}$;*Yap*$^{fl/fl}$;*Taz*$^{-/-}$ and control at 13.5dpc (sagittal) and 16.5dpc (frontal) showing the presence of SOX2+ cells in both genotypes. **C.** Immunofluorescence staining for SOX2, Endomucin (EMCN) and active YAP in P28 *Hesx1*$^{Cre/+}$;*Yap*$^{fl/fl}$;*Taz*$^{-/-}$ and control pituitaries, identifies SOX2+ cells in regions that are negative for active YAP (mice are null for TAZ) and normal vasculature. **D.** Graph quantifying the percentage of SOX2+ cells expressing active YAP in control and *Hesx1*$^{Cre/+}$;*Yap*$^{fl/fl}$;*Taz*$^{-/-}$ mutant pituitaries at P28. There is a reduction in double-positive cells in the mutant, which did not reach significance. **E.** Immunofluorescence staining for lineage committed progenitor markers PIT1 and SF1, as well as ACTH marking corticotrophs (TPIT lineage), reveals the presence and normal localisation of cells from the three lineages in a P28 *Hesx1*$^{Cre/+}$;*Yap*$^{fl/fl}$;*Taz*$^{-/-}$ mutant. Scale bars 100µm.

**Figure 2 – figure supplement 1 Pituitary-specific loss of *Stk3* and *Stk4* does not affect SOX2 cell specification or lineage commitment.**

**A.** Dorsal view of wholemount *Hesx1*$^{Cre/+}$;*Stk3*$^{fl/fl}$;*Stk4*$^{fl/fl}$ (mutant) and *Stk3*$^{fl/fl}$;*Stk4*$^{fl/fl}$ (control) pituitaries at P0 showing comparable morphology and size at birth. **B.** Western blot to determine levels of STK3 and STK4 proteins in *Hesx1*$^{Cre/+}$;*Stk3*$^{fl/fl}$;*Stk4*$^{fl/fl}$ mutant pituitaries compared to controls at P35, using an antibody against total STK3 and STK4 proteins. Comparison of STK3/4 band intensities confirms a significant reduction in mutants (Student's *t*-test, *P*=0.00032

(***)). STK3/4 bands normalised to the housekeeping protein Cyclophilin B. **C.** Immunofluorescence staining using antibodies against SOX2, TAZ, Endomucin (EMCN), YAP and pYAP at P0, indicating comparable staining between control and mutant samples. **D.** Immunofluorescence staining against lineage commitment markers PIT1, TPIT and SF1 shows normal lineage commitment in a *Hesx1*$^{Cre/+}$;*Stk3*$^{fl/fl}$;*Stk4*$^{fl/fl}$ mutant pituitary compared to the control at P10. **E.** Hematoxylin and eosin staining through frontal sections of *Hesx1*$^{Cre/+}$;*Stk3*$^{fl/fl}$;*Stk4*$^{fl/fl}$ and control pituitaries at P70. AL: anterior lobe, IL: intermediate lobe, PL: posterior lobe. Scale bars 100μm.

**Figure 2 – figure supplement 2 Isolated deletions of *Lats1* or *Lats2* in the pituitary do not affect development.**

**A.** Hematoxylin and eosin staining of a sagittal section of *Hesx1*$^{Cre/+}$;*Lats1*$^{fl/fl}$ at 13.5dpc showing normal morphology (see Figure 2A for control). Dashed lines demarcate developing Rathke's pouch. Immunofluorescence staining for TAZ and YAP reveals a normal expression pattern and no gross protein accumulation (compare to control, Figure 2A) **B.** Dorsal view of wholemount *Hesx1*$^{Cre/+}$;*Lats1*$^{fl/fl}$ (mutant) and *Hesx1*$^{Cre/+}$ (control) pituitaries at P0 showing comparable morphology and size at birth. **C.** RNAscope mRNA *in situ* hybridisation against *Lats2* shows an increase in transcripts in the anterior pituitary following deletion of *Lats1* (*Hesx1*$^{Cre/+}$;*Lats1*$^{fl/fl}$) compared to control (*Hesx1*$^{Cre/+}$), where *Lats2* expression is barely detectable**. D.** Hematoxylin and eosin staining of a sagittal section of *Hesx1*$^{Cre/+}$;*Lats2*$^{fl/fl}$ at 13.5dpc showing normal morphology (see Figure 2A for control). Dashed lines demarcate developing Rathke's pouch. **E.** Hematoxylin and eosin staining on frontal sections through 15.5dpc embryonic heads of *Hesx1*$^{Cre/+}$;*Lats1*$^{fl/fl}$;*Lats2*$^{fl/fl}$ (mutant) and control (*Hesx1*$^{+/+}$;*Lats1*$^{fl/fl}$;*Lats2*$^{fl/fl}$) genotypes, at the levels indicated in the cartoon. Note the hyperplastic pituitary at both axial levels, exerting mass effect on the brain. Asterisk indicates necrosis. Graph showing quantification of pituitary size at 15.5dpc as measured by the area occupied by the pituitary in matched histological sections between control and mutant embryos. *Hesx1*$^{Cre/+}$;*Lats1*$^{fl/fl}$;*Lats2*$^{fl/fl}$ mutant pituitaries are significantly larger (average 0.7195mm$^2$) compared to controls (average 0.1994mm$^2$) (Student's *t*-test, *P*=0.0003 (***)). **F.** Quantification of Ki-67+ and SOX9+ cells across the whole Rathke's pouch of *Hesx1*$^{Cre/+}$ (control) and *Hesx1*$^{Cre/+}$;*Lats1*$^{fl/fl}$ (mutant) pituitaries at 13.5dpc. There is a significant increase in

cycling cells in mutants, marked by Ki-67 (Student's *t*-test, *P*=0.0067 (**)). The proportion of SOX9+ cells is comparable between genotypes. Scale bars 100µm in A-D, 1mm in E.

**Figure 3 – figure supplement 1 Analysis of tumourigenic lesions in postnatal pituitaries following pituitary-specific deletion of *Lats1*.**

**A.** Immunofluorescence staining for TAZ and active YAP reveal lesions of accumulation at P21 in $Hesx1^{Cre/+};Lats1^{fl/fl};Lats2^{fl/+}$ compared to $Hesx1^{+/+};Lats1^{fl/fl};Lats2^{fl/+}$ control. Immunofluorescence staining using antibodies against SOX2 and Endomucin (EMCN) show these lesions are composed of SOX+ stem cells and have reduced vascularisation. **B.** Hematoxylin and eosin staining of frontal sections from $Hesx1^{Cre/+};Lats2^{fl/fl}$ and $Hesx1^{Cre/+}$ control pituitaries at P56 showing comparable histology. **C.** Immunofluorescence staining against SOX2 and Endomucin on an intermediate lobe lesion (asterisk) in a $Hesx1^{Cre/+};Lats1^{fl/fl};Lats2^{fl/+}$ pituitary compared to control. **D.** Immunofluorescence staining against DNA damage marker gamma H2A.X showing positive cells in $Hesx1^{Cre/+};Lats1^{fl/fl};Lats2^{fl/+}$ mutants. **E.** P56 Immunohistochemistry using antibodies against p63 and the AE1/AE3 cytokeratin cocktail, both positive in pituitary carcinomas, showing abundant staining in $Hesx1^{Cre/+};Lats1^{fl/fl};Lats2^{fl/+}$ compared to control. Note that membrane staining detected in controls is background for both antibodies. **F.** Immunohistochemistry using antibodies against synaptophysin, neural-specific enolase (NSE) and chromogranin demonstrate tumourigenic lesions in $Hesx1^{Cre/+};Lats1^{fl/fl};Lats2^{fl/+}$ are negative for adenoma markers. Lesions are negative for vimentin by immunofluorescence staining, commonly marking spindle-cell oncocytoma in the pituitary. Scale bars 100µm in A, C-F; 500µm in B. PL: posterior lobe, IL: intermediate lobe, AL: anterior lobe.

**Figure 4 – figure supplement 1 Analysis of tumourigenic lesions in postnatal pituitaries following SOX2-specific deletion of *Lats1*.**

**A.** Graph of quantification of lineage commitment markers PIT1, TPIT and SF1, as a percentage of all anterior pituitary cells, in $Sox2^{+/+};Lats1^{fl/fl};Lats2^{fl/+}$ (control) and $Sox2^{CreERT2/+};Lats1^{fl/fl};Lats2^{fl/+}$ (mutant) pituitaries. There is a significant reduction in the percentage of committed cells of all three lineages in mutants compared to controls (Student's *t*-test; PIT1: *P*<0.0001 (****), TPIT: *P*<0.0001 (****), SF1:

*P*=0.004 (**)). **B.** Immunohistochemistry using specific antibodies against p63 and cytokeratin cocktail AE1/AE3 on frontal sections of *Sox2*$^{CreERT2/+}$;*Lats1*$^{fl/fl}$;*Lats2*$^{fl/+}$ (mutant) and *Sox2*$^{+/+}$;*Lats1*$^{fl/fl}$;*Lats2*$^{fl/+}$ (control) pituitaries at P35, revealing positive staining in mutants. Note that the membrane staining in controls is background for both antibodies. **C.** Double immunofluorescence staining against total YAP and GFP, as well as SOX2 and GFP in consecutive sections of a tumourigenic lesion from *Sox2*$^{CreERT2/+}$;*Lats1*$^{fl/fl}$;*Lats2*$^{fl/+}$;R26$^{mTmG/+}$ pituitaries at P35. Lineage tracing of SOX2+ cells, detected using GFP reveals abundant staining in the tumour lesion, characterised by accumulation of YAP and SOX2+ cells (yellow arrowheads). Scale bars 100μm.

**Figure 5 – figure supplement 1 Postnatal expression of constitutively active YAP increases leads to an activation of SOX2+ pituitary stem cells.**

**A.** Schematic outlining the time course of doxycycline (DOX) treatment administered to *Hesx1*$^{Cre/+}$;*R26*$^{rtTA/+}$;*Col1a1*$^{tetO\text{-}Yap/+}$ (YAP-TetO) and *Hesx1*$^{+/+}$;*R26*$^{rtTA/+}$;*Col1a1*$^{tetO\text{-}Yap/+}$ controls to drive expression of YAP-S127A in mutant pituitaries. Hematoxylin and eosin staining of control and YAP-TetO pituitaries at P42 (3 weeks treatment), P63 (6 weeks treatment) and P105 (12 weeks treatment). **B.** RNAscope mRNA *in situ* hybridisation against YAP targets *Cyr61* and *Ctgf* showing increased transcripts in YAP-TetO sections compared to controls at P42. **C.** Analysis of YAP-TetO mutants at P105: double immunofluorescence staining against SOX2 and Ki-67 reveals regions of expanded SOX2+;Ki-67- cells compared to the normal expression pattern in the control. This region is SOX9+, does not accumulate TAZ or YAP and expresses pYAP as does normal anterior pituitary epithelium. Immunofluorescence against PIT1 shows the absence of commitment to this lineage, a pattern not seen in the control. Hematoxylin and eosin staining in consecutive sections identifies this region, which does not have neoplastic features. **D.** Schematic outlining the time course of doxycycline (DOX) treatment administered to *Hesx1*$^{Cre/+}$;*R26*$^{rtTA/+}$;*Col1a1*$^{tetO\text{-}Yap/+}$ (YAP-TetO) and *Hesx1*$^{+/+}$;*R26*$^{rtTA/+}$;*Col1a1*$^{tetO\text{-}Yap/+}$ controls to drive expression of YAP-S127A in mutant pituitaries for three weeks, followed by a three-week recovery period in the absence of DOX. Hematoxylin and eosin staining of control and YAP-TetO pituitaries. RNAscope mRNA *in situ* hybridisation shows comparable levels of expression of targets *Cyr61* and *Ctgf*. **E.** Graph comparing total fluorescence of *Cyr61* and *Ctgf* by Fast Red RNAscope

mRNA *in situ* hybridisation across sections from control, *Hesx1*$^{Cre/+}$;*R26*$^{rtTA/+}$;*Col1a1*$^{tetO\text{-}Yap/+}$ (YAP-TetO) and *Sox2*$^{CreERT2/+}$;*Lats1*$^{fl/fl}$;*Lats2*$^{fl/+}$ anterior pituitaries, normalised for total anterior pituitary area. There is a significant increase in the expression of both targets in *Sox2*$^{CreERT2/+}$;*Lats1*$^{fl/fl}$;*Lats2*$^{fl/+}$ pituitaries compared to other genotypes (one-way ANOVA with Tukey's post hoc test; Control v *Sox2*$^{CreERT2/+}$;*Lats1*$^{fl/fl}$;*Lats2*$^{fl/+}$: $P<0.0001$ for *Cyr61* (****), $P=0.001$ for *Ctgf* (***); YAP-TetO v *Sox2*$^{CreERT2/+}$;*Lats1*$^{fl/fl}$;*Lats2*$^{fl/+}$: $P<0.0001$ for *Cyr61* (****), $P=0.0049$ for *Ctgf* (**)). Scale bars 250µm in A, 100µm in B-D.

SUPPLEMENTARY FILE LEGENDS

**Supplementary File 1**

Table showing expected and observed frequency of genotypes from *Hesx1*$^{Cre/+}$;*Yap*$^{fl/fl}$;*Taz*$^{+/-}$ x *Yap*$^{fl/fl}$;*Taz*$^{+/-}$ at embryonic 15.5dpc and postnatal day 0-2. Embryonic: P=0.3471, Chi-square test (two tailed). Postnatal: P=0.0003 (***), Chi-square test (two tailed).

**Supplementary File 2**

Table showing expected and observed frequency of genotypes from *Hesx1*$^{Cre/+}$;*Lats1*$^{fl/+}$;*Lats2*$^{fl/+}$ x *Lats1*$^{fl/fl}$;*Lats2*$^{fl/fl}$ and *Hesx1*$^{Cre/+}$;*Lats1*$^{fl/+}$;*Lats2*$^{fl/+}$ x *Lats1*$^{fl/fl}$;*Lats2*$^{fl/+}$ at embryonic 15.5dpc and postnatal day 0-2. Embryonic: P<0.0001 (****), Chi-square test (two tailed). Postnatal: P<0.0001 (****), Chi-square test (two tailed).

References


1. Andoniadou CL*, et al.* Sox2(+) stem/progenitor cells in the adult mouse pituitary support organ homeostasis and have tumor-inducing potential. *Cell Stem Cell* **13**, 433-445 (2013).

2. Rizzoti K, Akiyama H, Lovell-Badge R. Mobilized adult pituitary stem cells contribute to endocrine regeneration in response to physiological demand. *Cell Stem Cell* **13**, 419-432 (2013).

3. Li S, Crenshaw EB, 3rd, Rawson EJ, Simmons DM, Swanson LW, Rosenfeld MG. Dwarf locus mutants lacking three pituitary cell types result from mutations in the POU-domain gene pit-1. *Nature* **347**, 528-533 (1990).

4. Pulichino AM, Vallette-Kasic S, Tsai JP, Couture C, Gauthier Y, Drouin J. Tpit determines alternate fates during pituitary cell differentiation. *Genes Dev* **17**, 738-747 (2003).

5. Ingraham HA*, et al.* The nuclear receptor steroidogenic factor 1 acts at multiple levels of the reproductive axis. *Genes Dev* **8**, 2302-2312 (1994).

6. Levy A. Physiological implications of pituitary trophic activity. *J Endocrinol* **174**, 147-155 (2002).

7. Nolan LA, Kavanagh E, Lightman SL, Levy A. Anterior pituitary cell population control: basal cell turnover and the effects of adrenalectomy and dexamethasone treatment. *J Neuroendocrinol* **10**, 207-215 (1998).

8. Bronstein MD, Paraiba DB, Jallad RS. Management of pituitary tumors in pregnancy. *Nat Rev Endocrinol* **7**, 301-310 (2011).

9. Daly AF, Rixhon M, Adam C, Dempegioti A, Tichomirowa MA, Beckers A. High prevalence of pituitary adenomas: a cross-sectional study in the province of Liege, Belgium. *J Clin Endocrinol Metab* **91**, 4769-4775 (2006).

10. Gonzalez-Meljem JM*, et al.* Stem cell senescence drives age-attenuated induction of pituitary tumours in mouse models of paediatric craniopharyngioma. *Nat Commun* **8**, 1819 (2017).

11. Lasolle H*, et al.* Temozolomide treatment can improve overall survival in aggressive pituitary tumors and pituitary carcinomas. *Eur J Endocrinol* **176**, 769-777 (2017).

12. Veldhuis JD. Changes in pituitary function with ageing and implications for patient care. *Nat Rev Endocrinol* **9**, 205-215 (2013).

13. Pernicone PJ*, et al.* Pituitary carcinoma: a clinicopathologic study of 15 cases. *Cancer* **79**, 804-812 (1997).

14. Heaney A. Management of aggressive pituitary adenomas and pituitary carcinomas. *J Neurooncol* **117**, 459-468 (2014).

15. Zhou D*, et al.* Mst1 and Mst2 maintain hepatocyte quiescence and suppress hepatocellular carcinoma development through inactivation of the Yap1 oncogene. *Cancer Cell* **16**, 425-438 (2009).

16. Lu L, Finegold MJ, Johnson RL. Hippo pathway coactivators Yap and Taz are required to coordinate mammalian liver regeneration. *Exp Mol Med* **50**, e423 (2018).

17. Zhou D*, et al.* Mst1 and Mst2 protein kinases restrain intestinal stem cell proliferation and colonic tumorigenesis by inhibition of Yes-associated protein (Yap) overabundance. *Proc Natl Acad Sci U S A* **108**, E1312-1320 (2011).

18. Lin C, Yao E, Chuang PT. A conserved MST1/2-YAP axis mediates Hippo signaling during lung growth. *Dev Biol* **403**, 101-113 (2015).

19. Nantie LB*, et al.* Lats inactivation reveals hippo function in alveolar type I cell differentiation during lung transition to air breathing. *Development*, (2018).

20. Meng Z, Moroishi T, Guan KL. Mechanisms of Hippo pathway regulation. *Genes Dev* **30**, 1-17 (2016).

21. Zhao B*, et al.* TEAD mediates YAP-dependent gene induction and growth control. *Genes Dev* **22**, 1962-1971 (2008).

22. Zhang H*, et al.* TEAD transcription factors mediate the function of TAZ in cell growth and epithelial-mesenchymal transition. *J Biol Chem* **284**, 13355-13362 (2009).

23. Zhou Y, Huang T, Cheng AS, Yu J, Kang W, To KF. The TEAD Family and Its Oncogenic Role in Promoting Tumorigenesis. *Int J Mol Sci* **17**, (2016).

24. Camargo FD*, et al.* YAP1 increases organ size and expands undifferentiated progenitor cells. *Curr Biol* **17**, 2054-2060 (2007).

25. Schlegelmilch K*, et al.* Yap1 acts downstream of alpha-catenin to control epidermal proliferation. *Cell* **144**, 782-795 (2011).

26. Dong J*, et al.* Elucidation of a universal size-control mechanism in Drosophila and mammals. *Cell* **130**, 1120-1133 (2007).

27. Lodge EJ, Russell JP, Patist AL, Francis-West P, Andoniadou CL. Expression Analysis of the Hippo Cascade Indicates a Role in Pituitary Stem Cell Development. *Front Physiol* **7**, 114 (2016).

28. Xekouki P*, et al.* Non-secreting pituitary tumours characterised by enhanced expression of YAP/TAZ. *Endocr Relat Cancer*, (2018).

29. Sheng HZ*, et al.* Specification of pituitary cell lineages by the LIM homeobox gene Lhx3. *Science* **272**, 1004-1007 (1996).

30. Tian Y*, et al.* TAZ promotes PC2 degradation through a SCFbeta-Trcp E3 ligase complex. *Mol Cell Biol* **27**, 6383-6395 (2007).

31. Moroishi T*, et al.* A YAP/TAZ-induced feedback mechanism regulates Hippo pathway homeostasis. *Genes Dev* **29**, 1271-1284 (2015).

32. Lavado A*, et al.* The Hippo Pathway Prevents YAP/TAZ-Driven Hypertranscription and Controls Neural Progenitor Number. *Developmental Cell*.

33. Andoniadou CL*, et al.* Identification of novel pathways involved in the pathogenesis of human adamantinomatous craniopharyngioma. *Acta Neuropathol* **124**, 259-271 (2012).

34. Sajedi E*, et al.* Analysis of mouse models carrying the I26T and R160C substitutions in the transcriptional repressor HESX1 as models for septo-optic dysplasia and hypopituitarism. *Dis Model Mech* **1**, 241-254 (2008).

35. Gaston-Massuet C*, et al.* Genetic interaction between the homeobox transcription factors HESX1 and SIX3 is required for normal pituitary development. *Dev Biol* **324**, 322-333 (2008).

36. Pefani DE*, et al.* RASSF1A-LATS1 signalling stabilizes replication forks by restricting CDK2-mediated phosphorylation of BRCA2. *Nat Cell Biol* **16**, 962-971, 961-968 (2014).

37. Ahmed AA, Mohamed AD, Gener M, Li W, Taboada E. YAP and the Hippo pathway in pediatric cancer. *Mol Cell Oncol* **4**, e1295127 (2017).

38. Lee JH, Kavanagh JJ, Wildrick DM, Wharton JT, Blick M. Frequent loss of heterozygosity on chromosomes 6q, 11, and 17 in human ovarian carcinomas. *Cancer Res* **50**, 2724-2728 (1990).

39. Chen CF, Yeh SH, Chen DS, Chen PJ, Jou YS. Molecular genetic evidence supporting a novel human hepatocellular carcinoma tumor suppressor locus at 13q12.11. *Genes Chromosomes Cancer* **44**, 320-328 (2005).

40. Theile M*, et al.* A defined chromosome 6q fragment (at D6S310) harbors a putative tumor suppressor gene for breast cancer. *Oncogene* **13**, 677-685 (1996).

41. Mazurenko N*, et al.* High resolution mapping of chromosome 6 deletions in cervical cancer. *Oncol Rep* **6**, 859-863 (1999).

42. St John MA*, et al.* Mice deficient of Lats1 develop soft-tissue sarcomas, ovarian tumours and pituitary dysfunction. *Nature genetics* **21**, 182-186 (1999).

43. Hu JK, Du W, Shelton SJ, Oldham MC, DiPersio CM, Klein OD. An FAK-YAP-mTOR Signaling Axis Regulates Stem Cell-Based Tissue Renewal in Mice. *Cell Stem Cell* **21**, 91-106 e106 (2017).

44. Saeger W, Ludecke DK, Buchfelder M, Fahlbusch R, Quabbe HJ, Petersenn S. Pathohistological classification of pituitary tumors: 10 years of experience with the German Pituitary Tumor Registry. *Eur J Endocrinol* **156**, 203-216 (2007).

45. Lewis AJ, Cooper PW, Kassel EE, Schwartz ML. Squamous cell carcinoma arising in a suprasellar epidermoid cyst. Case report. *J Neurosurg* **59**, 538-541 (1983).

46. O'Neill BT, Segkos K, Kasper EM, Pallotta JA. Non-metastatic squamous cell carcinoma within a Rathke's cleft cyst. *Pituitary* **19**, 105-109 (2016).

47. Basu-Roy U*, et al.* Sox2 antagonizes the Hippo pathway to maintain stemness in cancer cells. *Nat Commun* **6**, 6411 (2015).

48. Panciera T*, et al.* Induction of Expandable Tissue-Specific Stem/Progenitor Cells through Transient Expression of YAP/TAZ. *Cell Stem Cell*, (2016).

49. Han ZY*, et al.* The occurrence of intracranial rhabdoid tumours in mice depends on temporal control of Smarcb1 inactivation. *Nat Commun* **7**, 10421 (2016).

50. Papaspyropoulos A*, et al.* RASSF1A uncouples Wnt from Hippo signalling and promotes YAP mediated differentiation via p73. *Nat Commun* **9**, 424 (2018).

51. Heallen T*, et al.* Hippo pathway inhibits Wnt signaling to restrain cardiomyocyte proliferation and heart size. *Science* **332**, 458-461 (2011).

52. Totaro A*, et al.* YAP/TAZ link cell mechanics to Notch signalling to control epidermal stem cell fate. *Nat Commun* **8**, 15206 (2017).

53. Zhu X, Tollkuhn J, Taylor H, Rosenfeld MG. Notch-Dependent Pituitary SOX2(+) Stem Cells Exhibit a Timed Functional Extinction in Regulation of the Postnatal Gland. *Stem Cell Reports* **5**, 1196-1209 (2015).

54. Nantie LB, Himes AD, Getz DR, Raetzman LT. Notch signaling in postnatal pituitary expansion: proliferation, progenitors, and cell specification. *Mol Endocrinol* **28**, 731-744 (2014).

55. Cheung LY, Rizzoti K, Lovell-Badge R, Le Tissier PR. Pituitary phenotypes of mice lacking the notch signalling ligand delta-like 1 homologue. *J Neuroendocrinol* **25**, 391-401 (2013).

56. Batchuluun K, Azuma M, Fujiwara K, Yashiro T, Kikuchi M. Notch Signaling and Maintenance of SOX2 Expression in Rat Anterior Pituitary Cells. *Acta Histochem Cytochem* **50**, 63-69 (2017).

57. Andoniadou CL*, et al.* Lack of the murine homeobox gene Hesx1 leads to a posterior transformation of the anterior forebrain. *Development* **134**, 1499-1508 (2007).

58. Muzumdar MD, Tasic B, Miyamichi K, Li L, Luo L. A global double-fluorescent Cre reporter mouse. *Genesis* **45**, 593-605 (2007).

59. Yu HM, Liu B, Chiu SY, Costantini F, Hsu W. Development of a unique system for spatiotemporal and lineage-specific gene expression in mice. *Proc Natl Acad Sci U S A* **102**, 8615-8620 (2005).

60. Jansson L, Larsson J. Normal hematopoietic stem cell function in mice with enforced expression of the Hippo signaling effector YAP1. *PLoS One* **7**, e32013 (2012).

61. Lu L*, et al.* Hippo signaling is a potent in vivo growth and tumor suppressor pathway in the mammalian liver. *Proceedings of the National Academy of Sciences* **107**, 1437-1442 (2010).

62. Schindelin J*, et al.* Fiji: an open-source platform for biological-image analysis. *Nat Methods* **9**, 676-682 (2012).

A

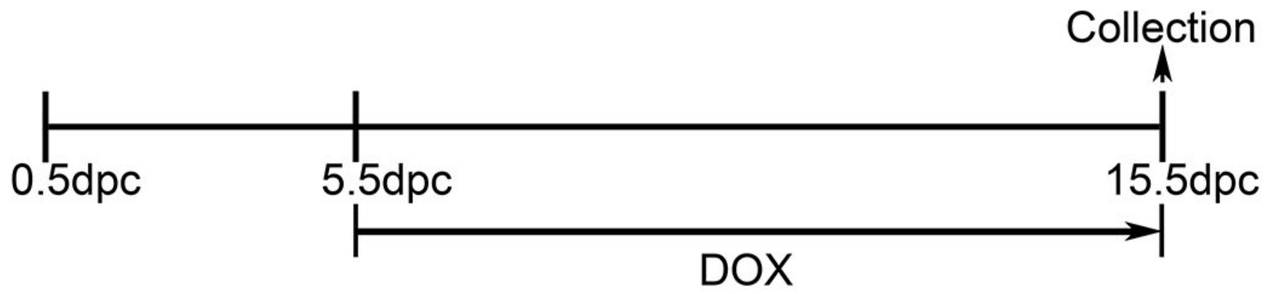


*Hesx1*$^{Cre/+}$;*R26*$^{rtTA/+}$;*Col1a1*$^{tetO\text{-}Yap/+}$
(YAP-TetO)

B

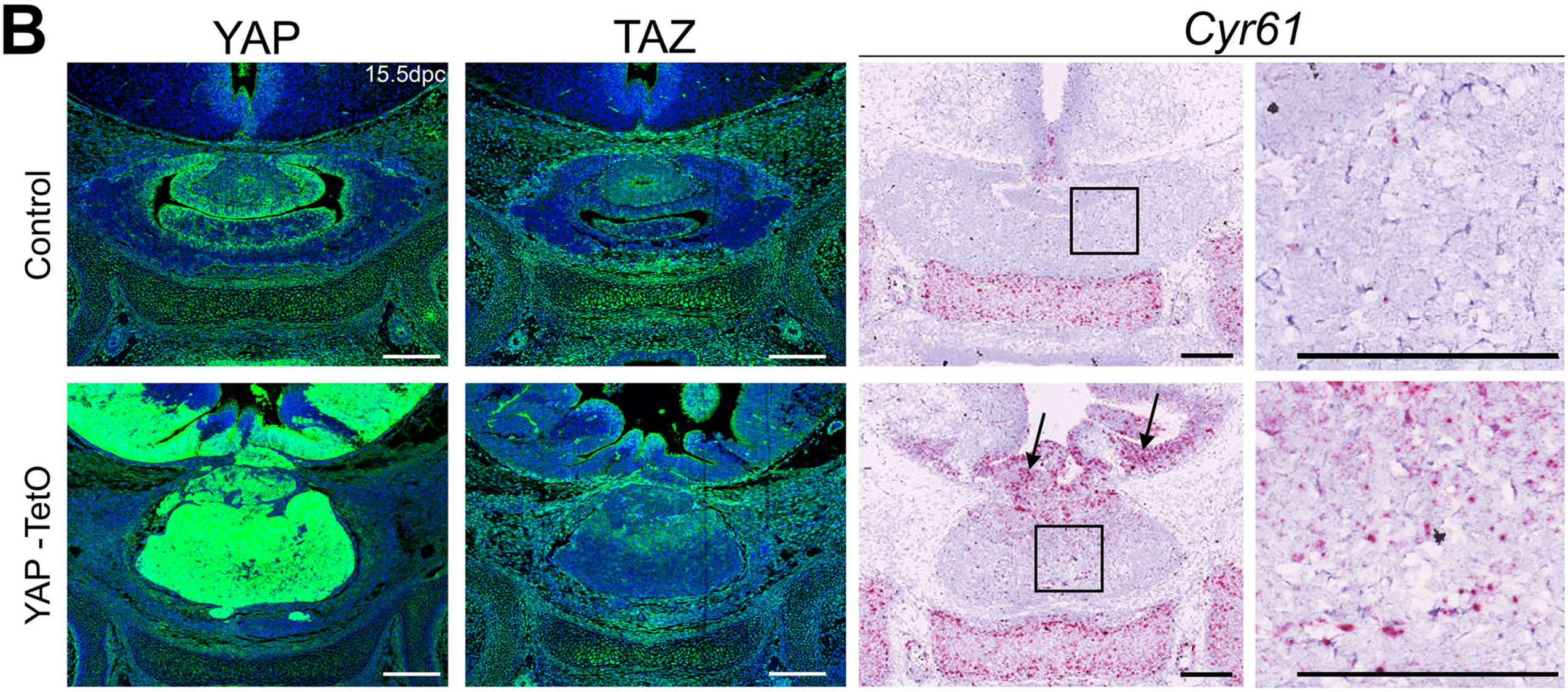


C

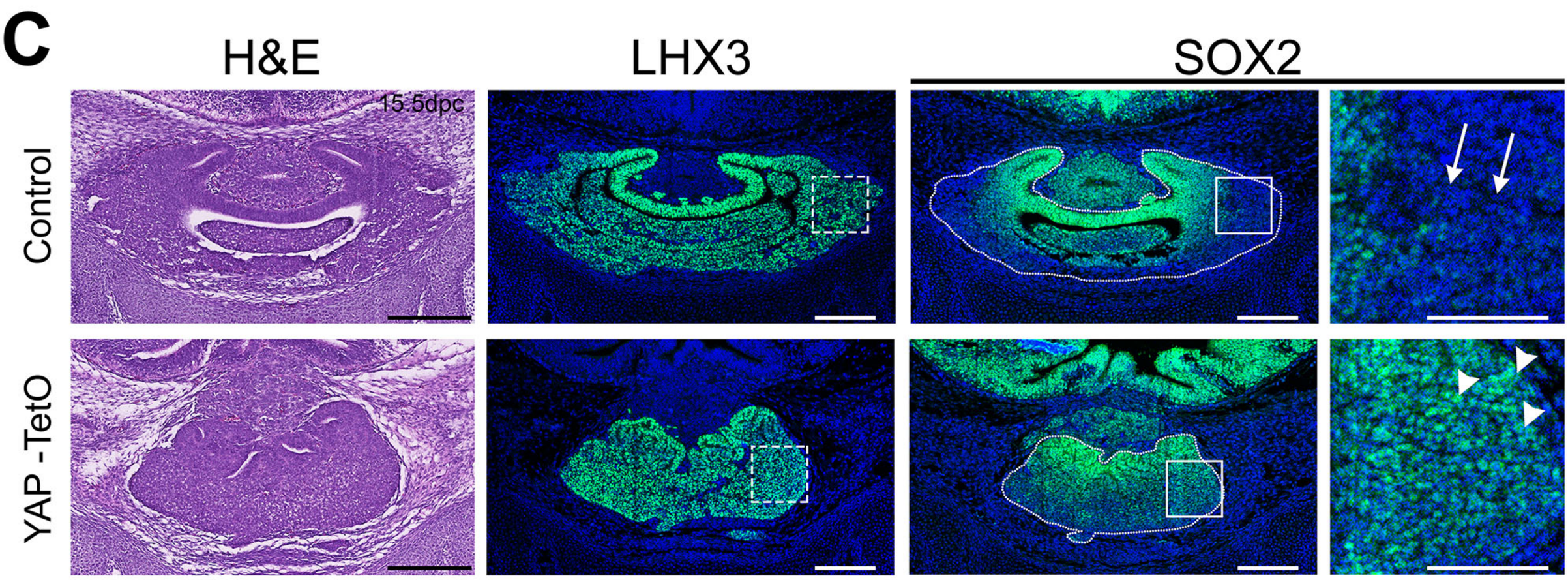


D

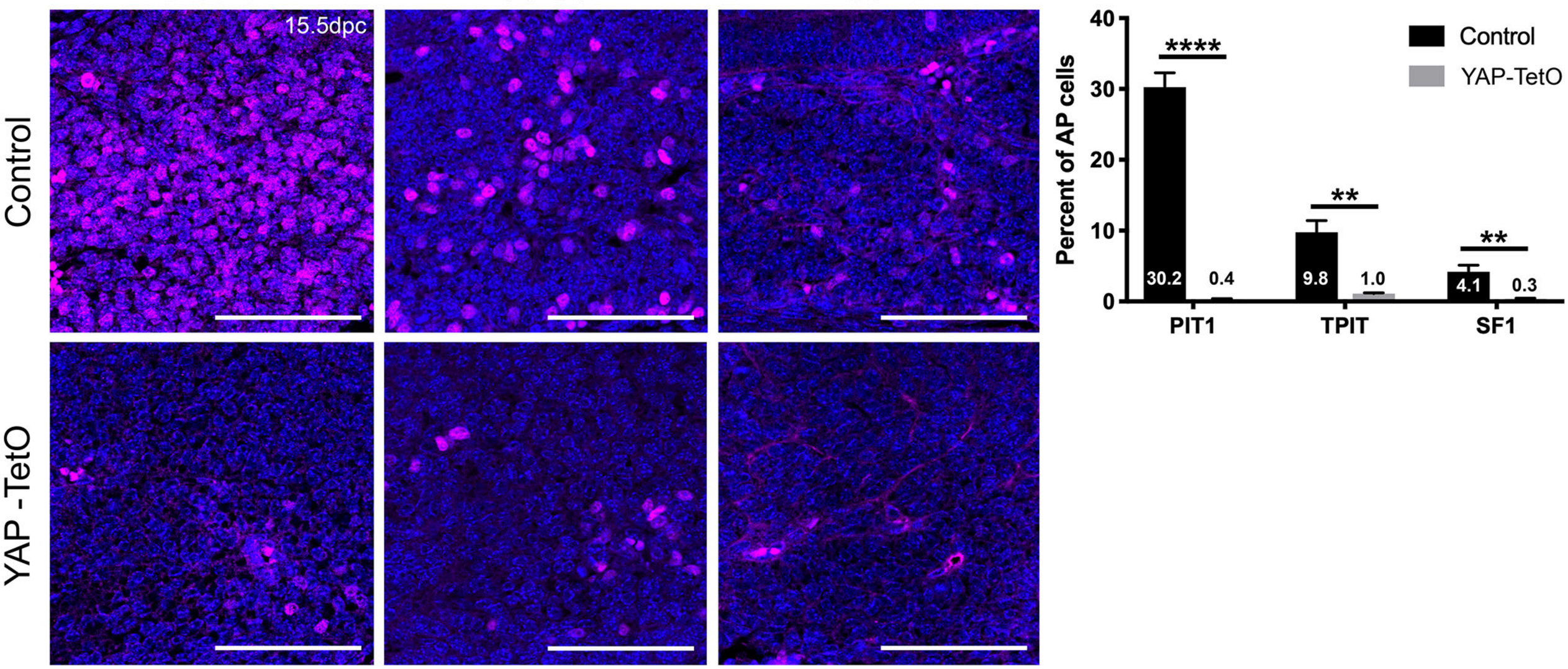

A

TAZ

YAP

pYAP

SOX2

Control

13.5 dpc

*Hesx1*$^{Cre/+}$;*Lats1*$^{fl/fl}$;
*Lats2*$^{fl/fl}$

B

SOX9

Ki-67

Control

13.5 dpc

*Hesx1*$^{Cre/+}$;*Lats1*$^{fl/fl}$;
*Lats2*$^{fl/fl}$

C

SOX2 / EMCN

Active YAP

Control

15.5 dpc

*Hesx1*$^{Cre/+}$;*Lats1*$^{fl/fl}$;
*Lats2*$^{fl/fl}$

D

PIT1

TPIT

SF1

Control

15.5 dpc

*Hesx1*$^{Cre/+}$;*Lats1*$^{fl/fl}$;*Lats2*$^{fl/fl}$

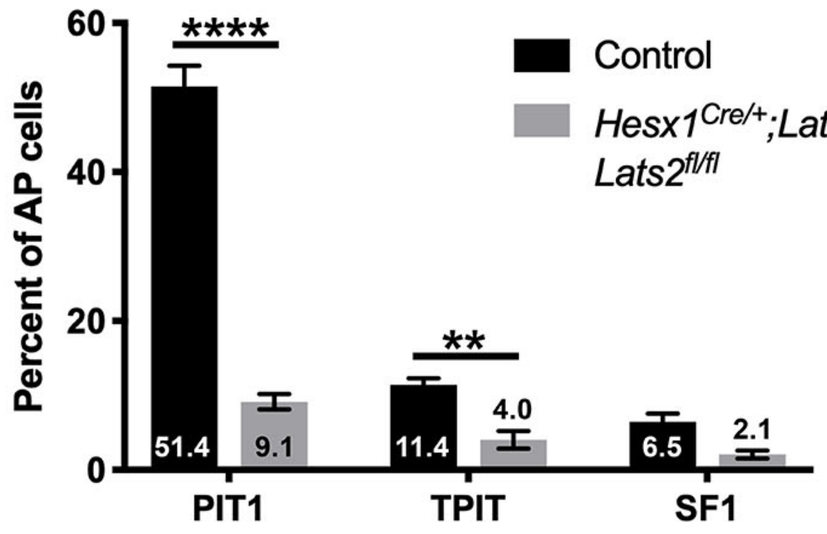

A

Control

*Hesx1*$^{Cre/+}$;*Lats1*$^{fl/fl}$;*Lats2*$^{fl/+}$

C

Ki-67

Percent Ki-67+ Cells / Total Cells

30
20
10
0

*

Control

*Hesx1*$^{Cre/+}$;*Lats1*$^{fl/fl}$; *Lats2*$^{fl/+}$

Control

*Hesx1*$^{Cre/+}$;*Lats1*$^{fl/fl}$; *Lats2*$^{fl/+}$

B

TAZ | YAP | pYAP | *Ctgf* | *Cyr61*

Control

*Hesx1*$^{Cre/+}$;*Lats1*$^{fl/fl}$; *Lats2*$^{fl/+}$

D

PIT1 | TPIT | SF1

Control

*Hesx1*$^{Cre/+}$;*Lats1*$^{fl/fl}$;*Lats2*$^{fl/+}$

E

SOX2 / EMCN | SOX9

Control

*Hesx1*$^{Cre/+}$;*Lats1*$^{fl/fl}$;*Lats2*$^{fl/+}$

F

*Hesx1*$^{Cre/+}$;*Lats1*$^{fl/fl}$; *Lats2*$^{fl/+}$

H&E

SOX2

A

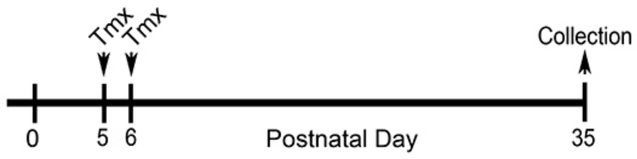


Control

$Sox2^{CreERT2/+};Lats1^{fl/fl};Lats2^{fl/+}$

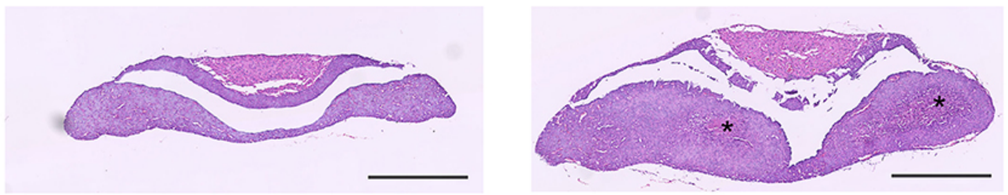

B

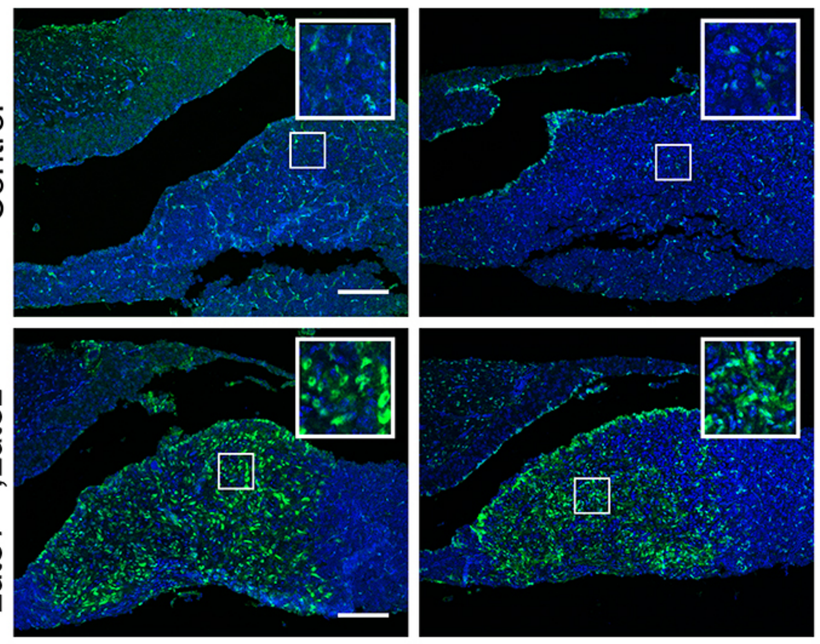


C

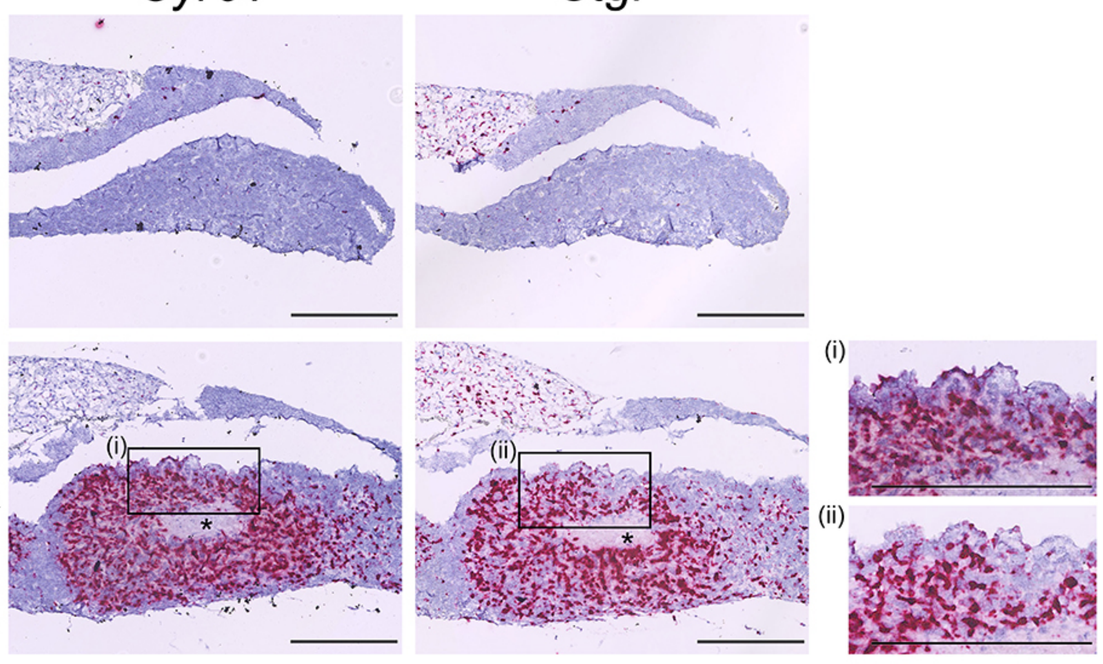


D

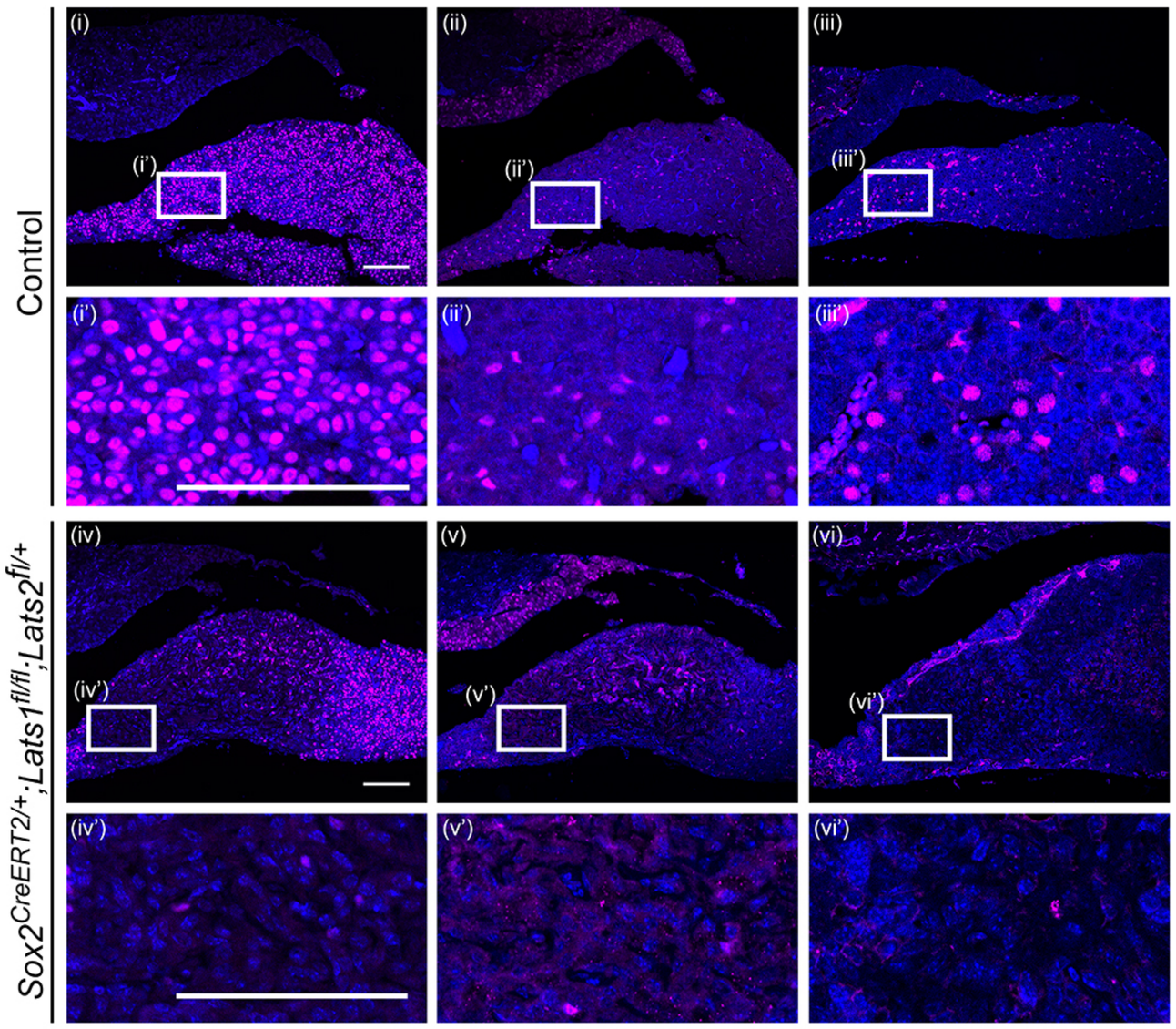


E

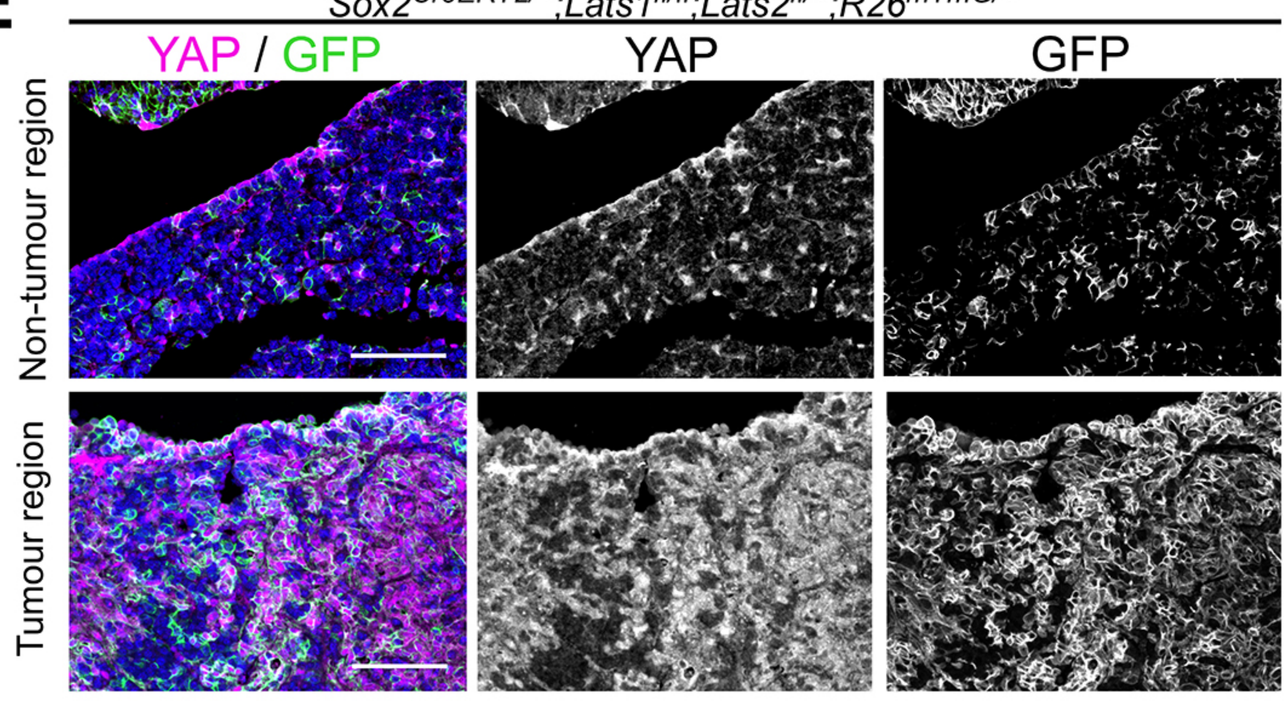

A

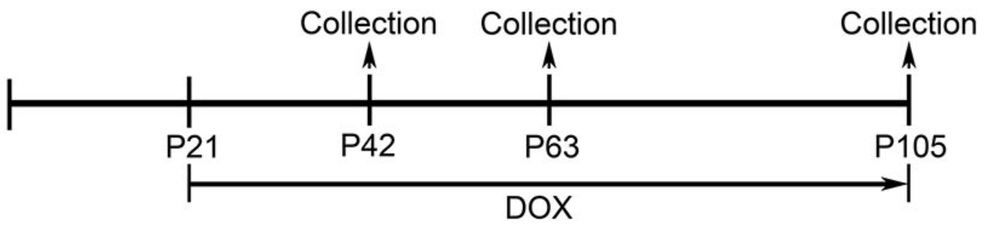


*Hesx1*$^{Cre/+}$;*R26*$^{rtTA/+}$;
*Col1a1*$^{tetO\text{-}Yap/+}$
(YAP-TetO)

B

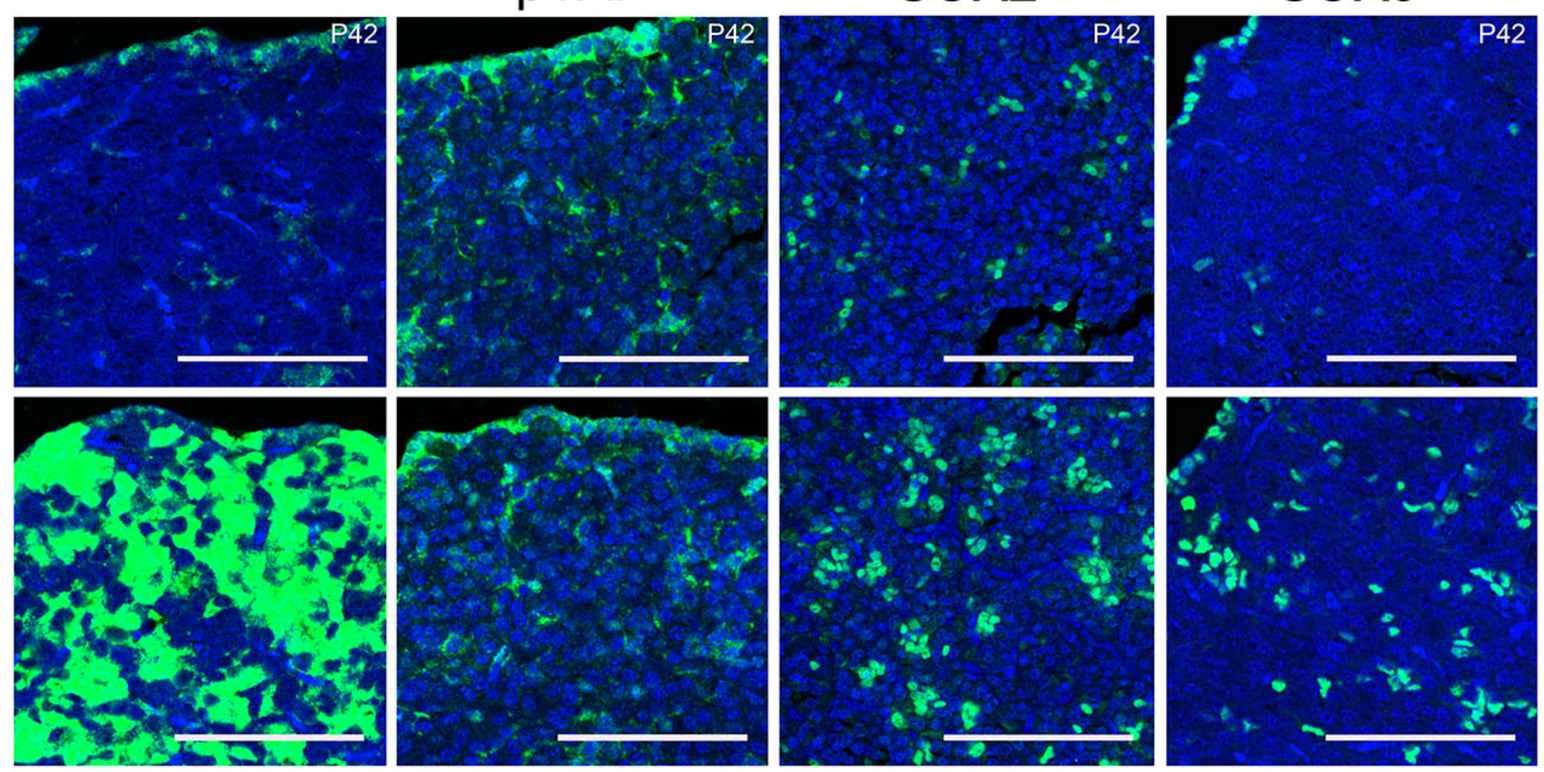


C

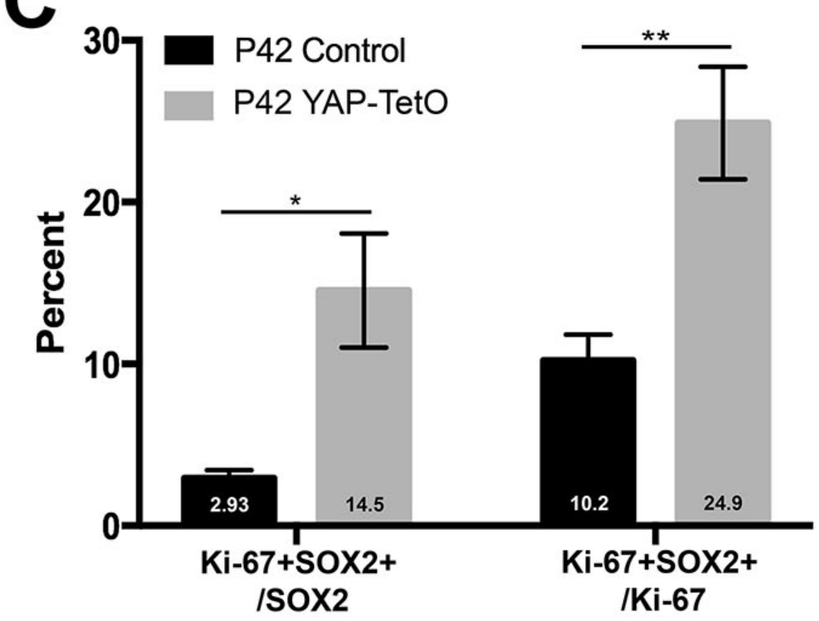


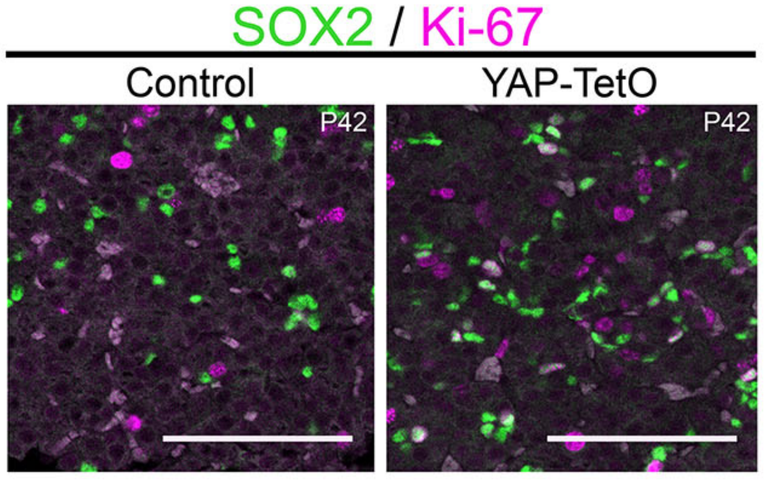


D

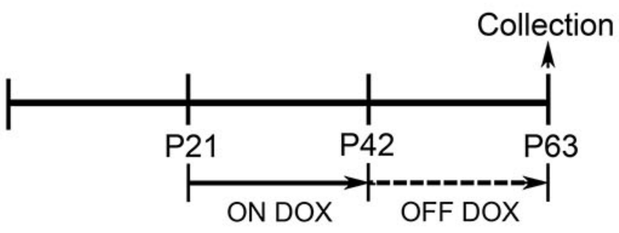


*Hesx1*$^{Cre/+}$;*R26*$^{rtTA/+}$;
*Col1a1*$^{tetO\text{-}Yap/+}$
(YAP-TetO) **Recovery**

E

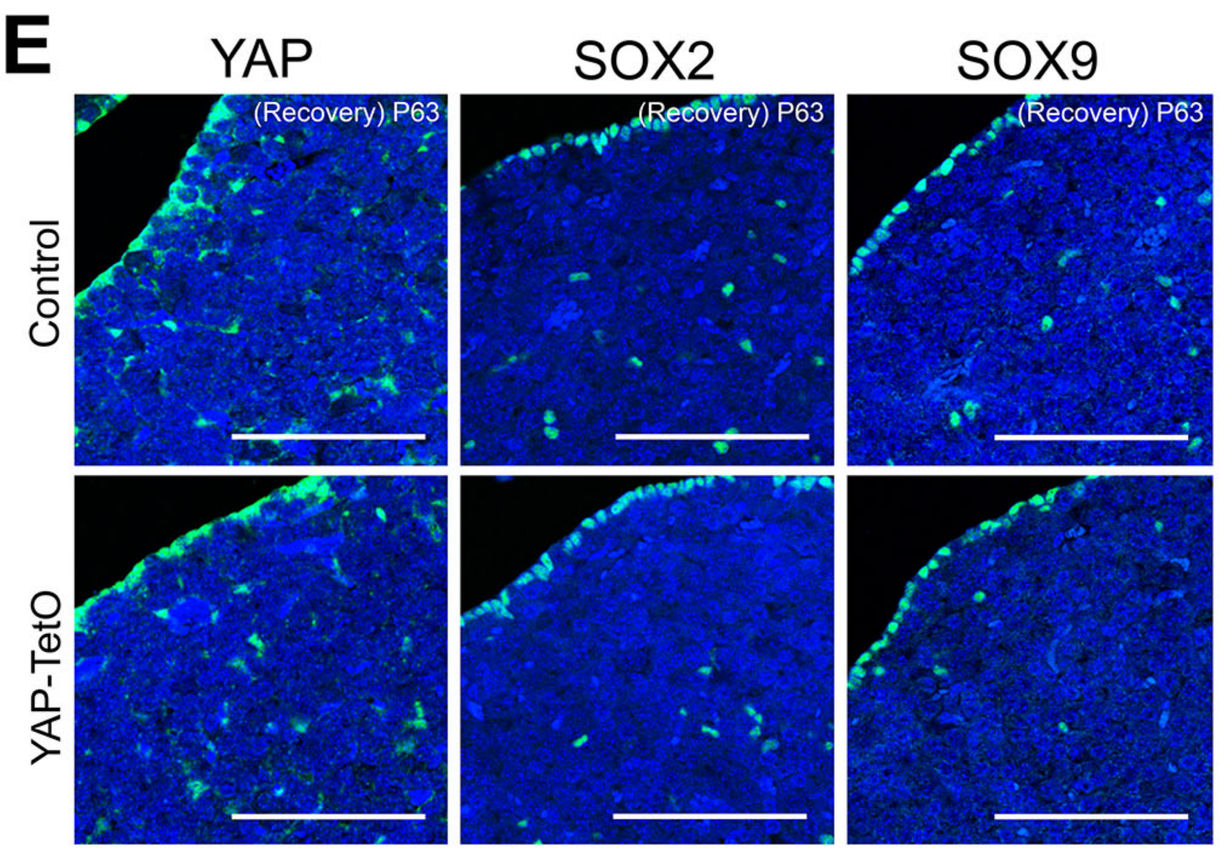


F

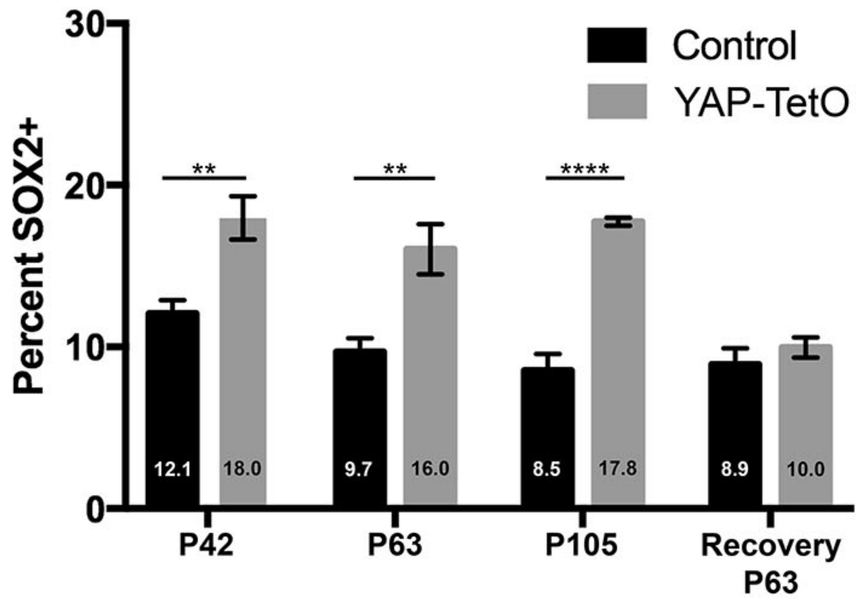


G

*Sox2*$^{CreERT2/+}$;*R26*$^{rtTA/mTmG}$;*Col1a1*$^{tetO\text{-}Yap/+}$
**Recovery**

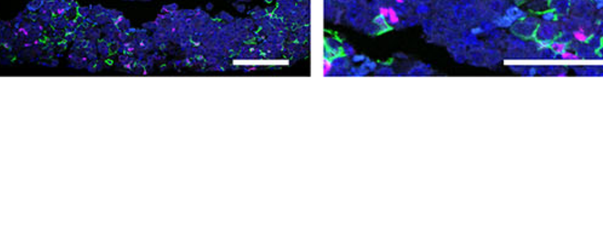


H

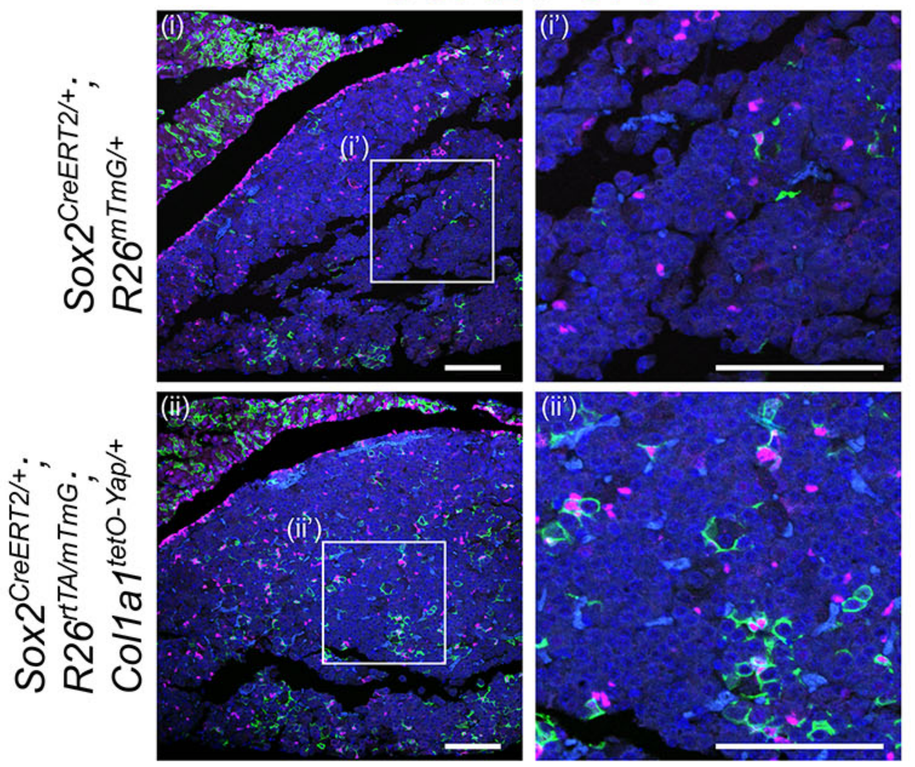


I

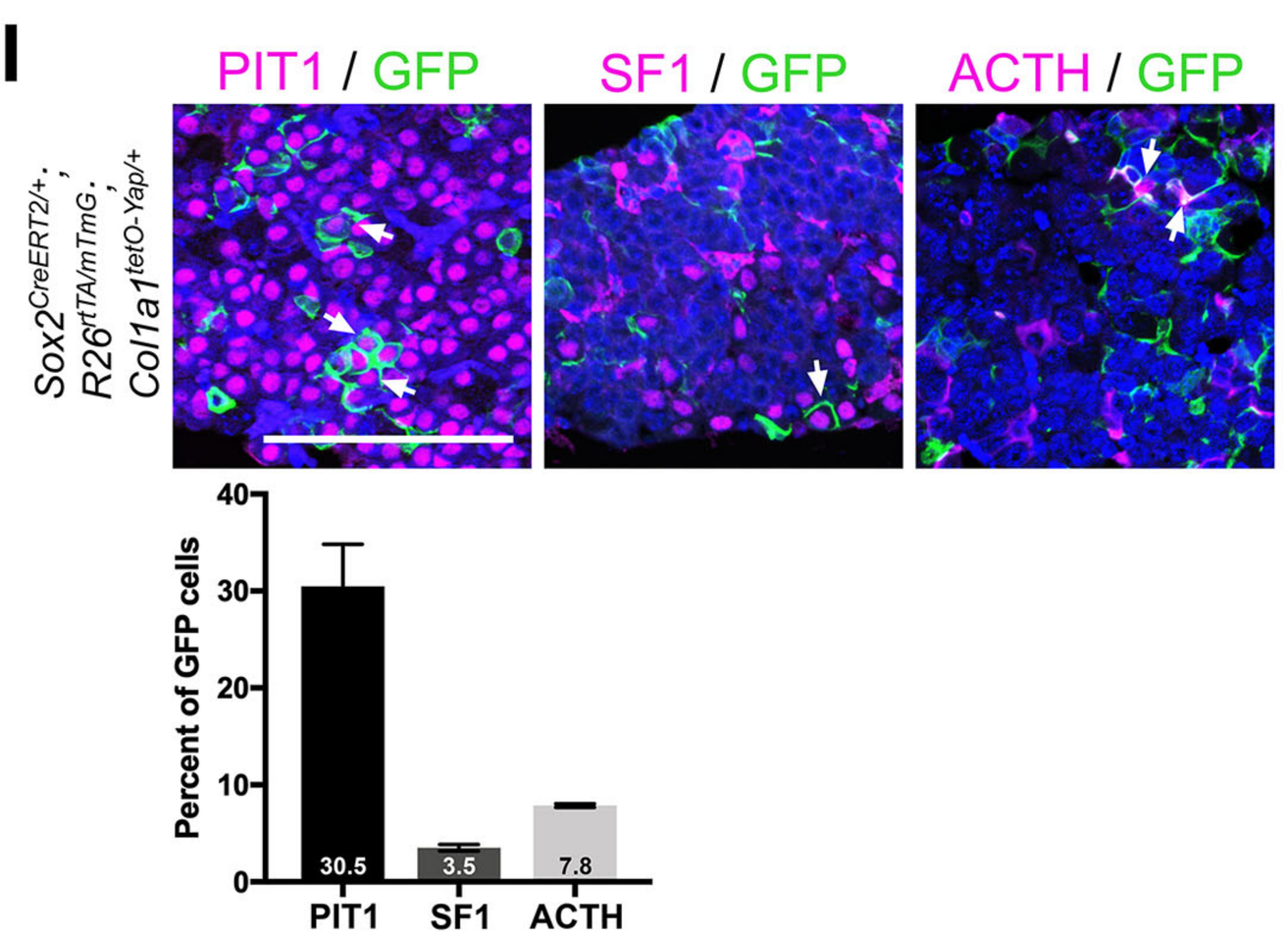

Normal regulation

Balanced maintenance of stem cell and endocrine cell pools

$SOX2^+$
$YAP^+$
$TAZ^+$

+YAP S127A
↑target genes

Stem cell expansion

+~~YAP S127A~~

Commitment of expanded population

~~LATS~~ (↑YAP/TAZ)
↑↑target genes

Tumour formation

KEY

Stem cell

Lineage-committed endocrine cells

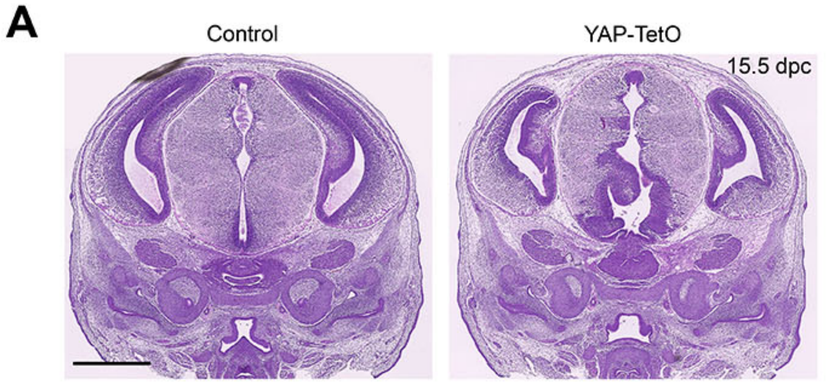
A
Control
YAP-TetO
15.5 dpc

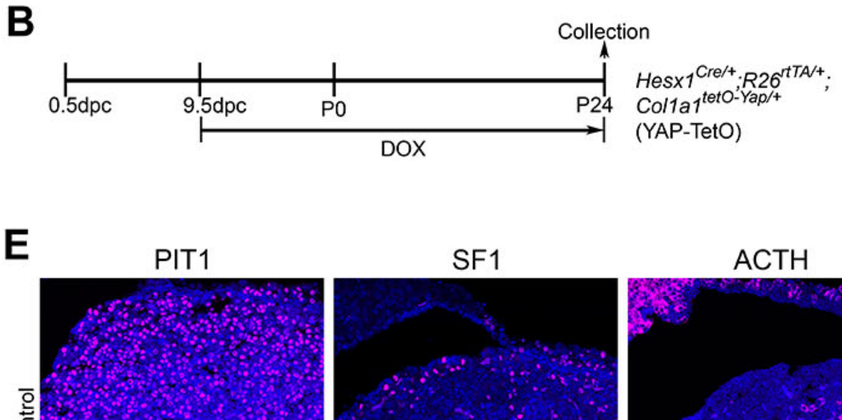
B
Collection
0.5dpc
9.5dpc
P0
P24
DOX
Hesx1Cre/+;R26rtTA/+;
Col1a1tetO-Yap/+
(YAP-TetO)

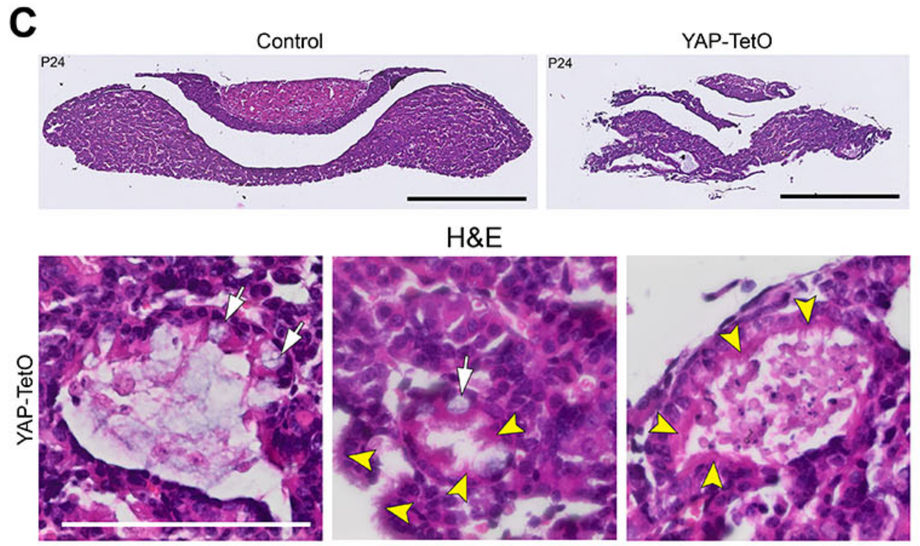
C
Control
YAP-TetO
P24
P24
H&E
YAP-TetO

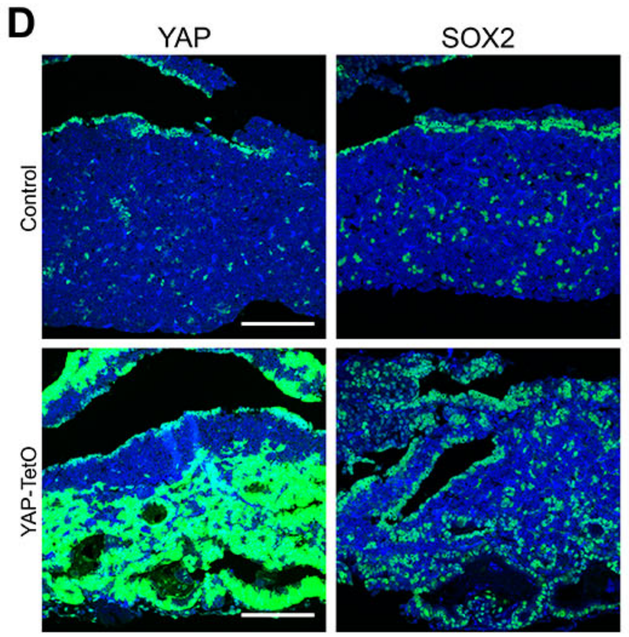
D
YAP
SOX2
Control
YAP-TetO

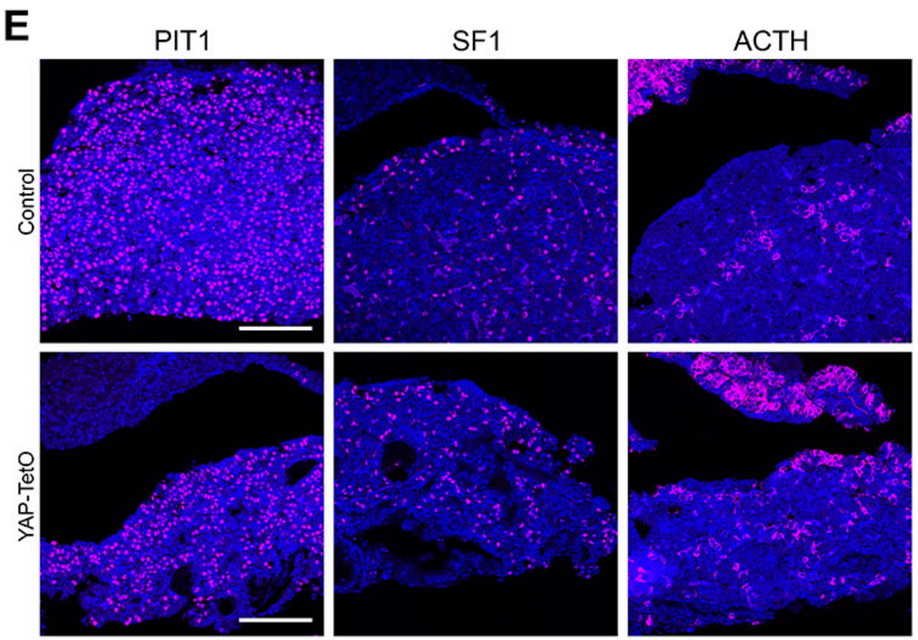
E
PIT1
SF1
ACTH
Control
YAP-TetO

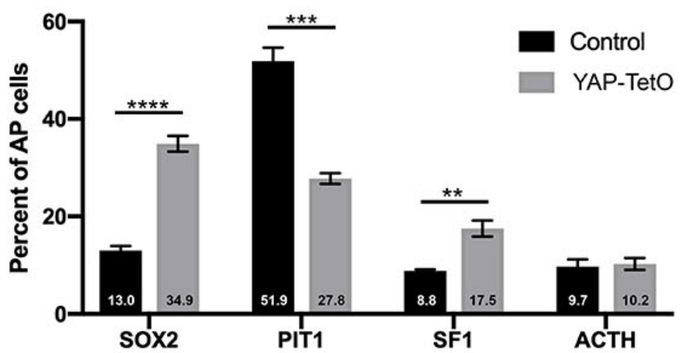
Percent of AP cells
60
40
20
0
****
***
**
Control
YAP-TetO
13.0
34.9
51.9
27.8
8.8
17.5
9.7
10.2
SOX2
PIT1
SF1
ACTH

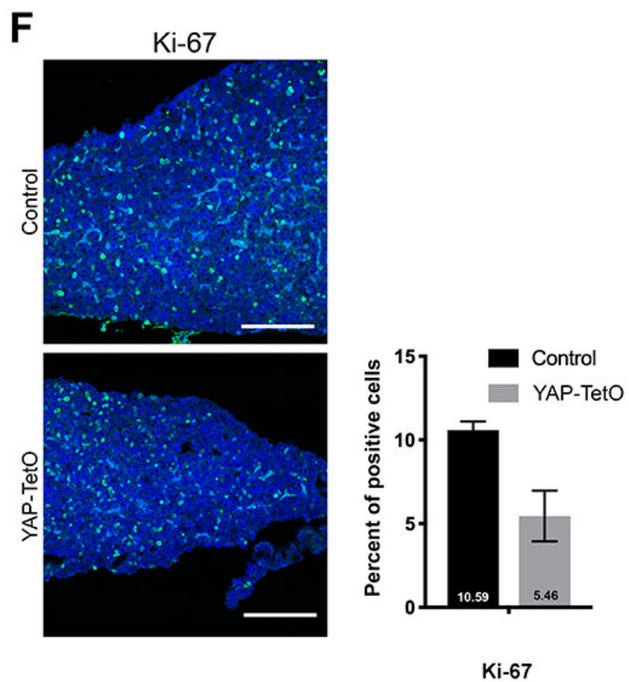
F
Ki-67
Control
YAP-TetO
Percent of positive cells
15
10
5
0
Control
YAP-TetO
10.59
5.46
Ki-67

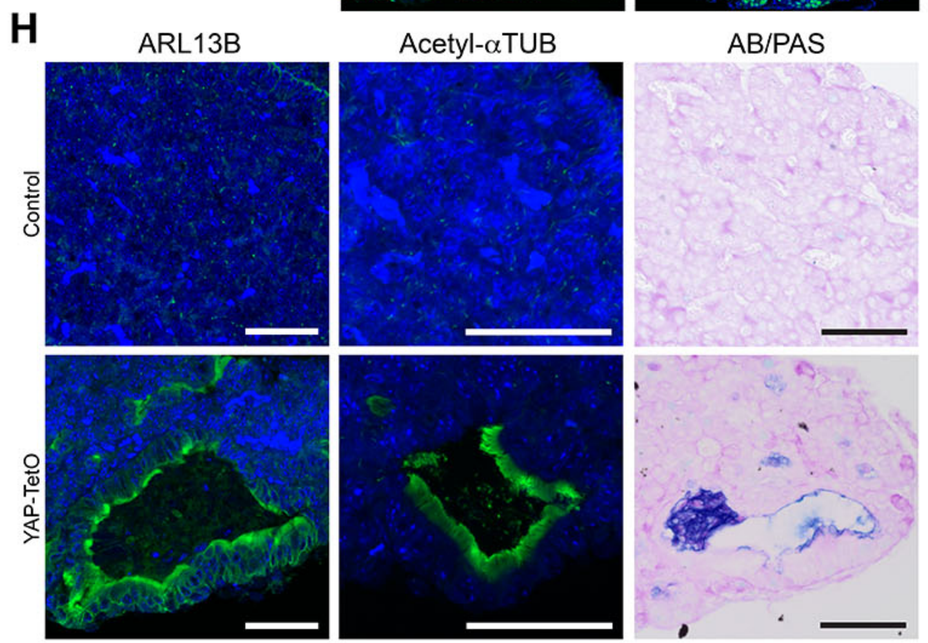
H
ARL13B
Acetyl-αTUB
AB/PAS
Control
YAP-TetO

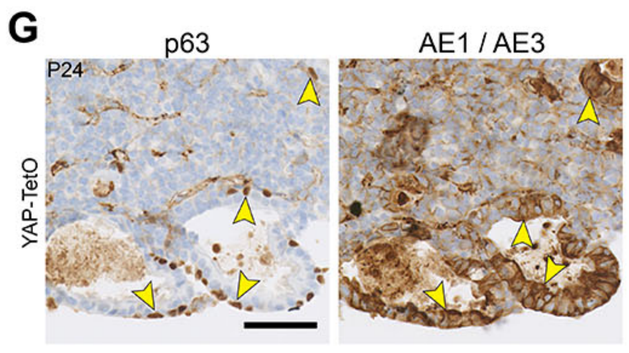
G
p63
AE1 / AE3
P24
YAP-TetO

A

H&E

13.5 dpc

Control

*Hesx1*$^{Cre/+}$;*Yap*$^{fl/fl}$;
*Taz*$^{-/-}$

B

SOX2

13.5 dpc

16.5 dpc

Control

*Hesx1*$^{Cre/+}$;*Yap*$^{fl/fl}$;
*Taz*$^{-/-}$

C

SOX2 / EMCN

Active YAP

P28

Control

*Hesx1*$^{Cre/+}$;*Yap*$^{fl/fl}$;
*Taz*$^{-/-}$

D

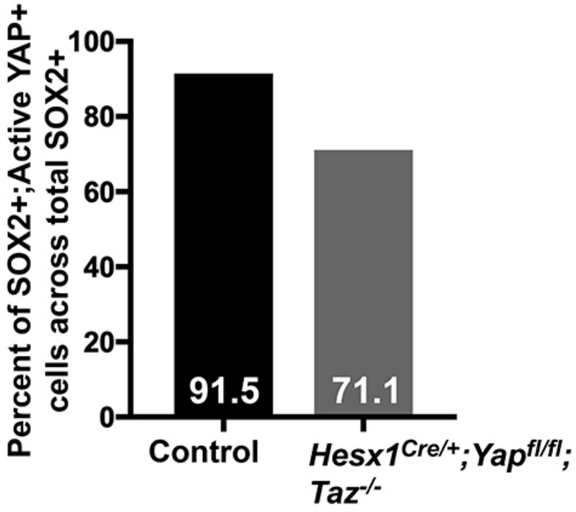


E

PIT1

SF1

ACTH

P28

Control

*Hesx1*$^{Cre/+}$;*Yap*$^{fl/fl}$;
*Taz*$^{-/-}$

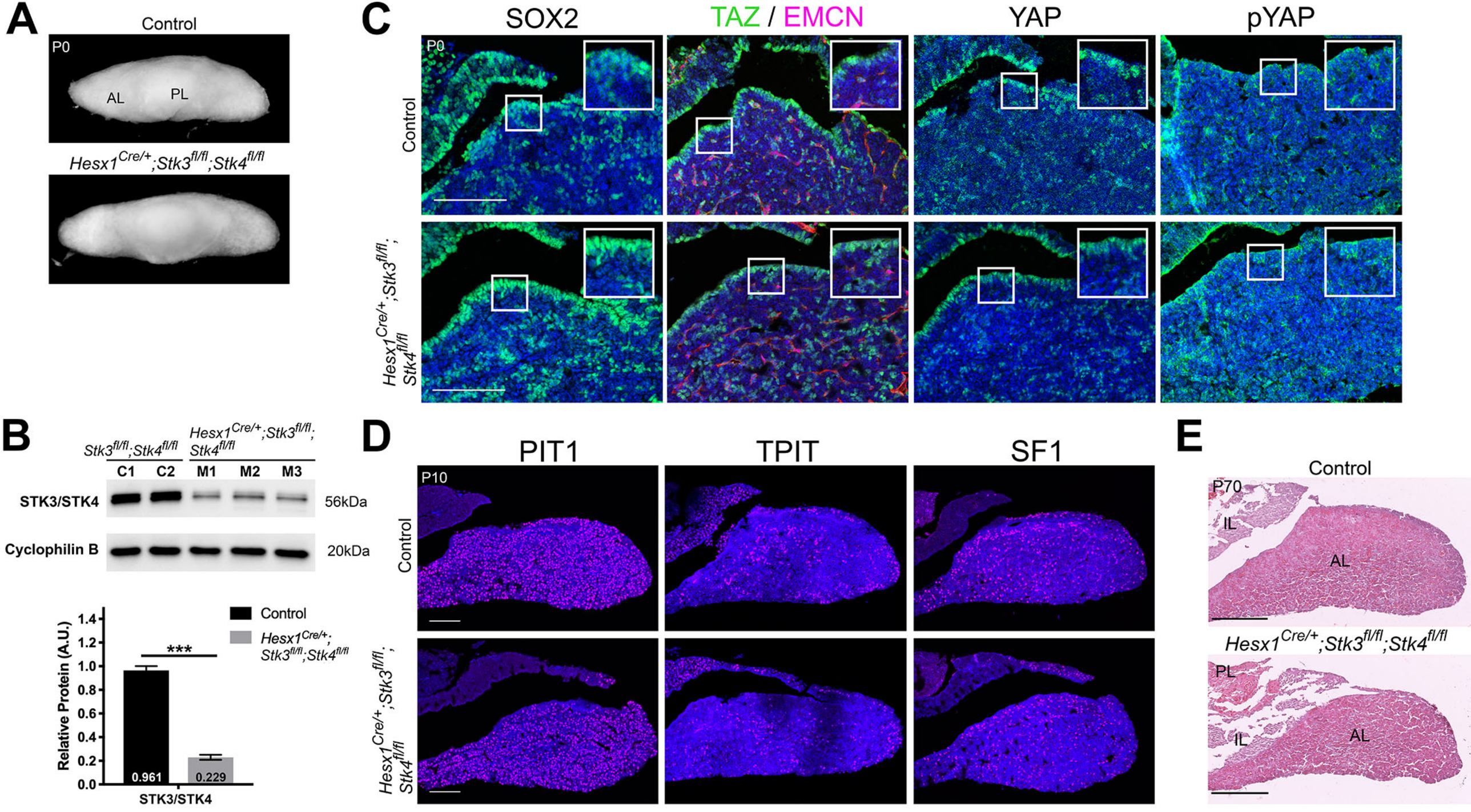
A
Control
P0
AL
PL
Hesx1Cre/+;Stk3fl/fl;Stk4fl/fl
B
Stk3fl/fl;Stk4fl/fl
Hesx1Cre/+;Stk3fl/fl;Stk4fl/fl
C1
C2
M1
M2
M3
STK3/STK4
56kDa
Cyclophilin B
20kDa
Relative Protein (A.U.)
1.4
1.2
1.0
0.8
0.6
0.4
0.2
0.0
***
Control
Hesx1Cre/+;Stk3fl/fl;Stk4fl/fl
0.961
0.229
STK3/STK4
C
SOX2
TAZ / EMCN
YAP
pYAP
P0
Control
Hesx1Cre/+;Stk3fl/fl;Stk4fl/fl
D
PIT1
TPIT
SF1
P10
Control
Hesx1Cre/+;Stk3fl/fl;Stk4fl/fl
E
Control
P70
IL
AL
Hesx1Cre/+;Stk3fl/fl;Stk4fl/fl
PL
IL
AL

A

*Hesx1*$^{Cre/+}$;*Lats1*$^{fl/fl}$

13.5 dpc

TAZ

YAP

B

Control

P0

*Hesx1*$^{Cre/+}$;*Lats1*$^{fl/fl}$

C

Control

*Hesx1*$^{Cre/+}$;*Lats1*$^{fl/fl}$

*Lats2*

D

*Hesx1*$^{Cre/+}$;*Lats2*$^{fl/fl}$

E

(i)

(ii)

15.5 dpc

Control

*Hesx1*$^{Cre/+}$;*Lats1*$^{fl/fl}$;
*Lats2*$^{fl/fl}$

***

Area mm²

1.0
0.8
0.6
0.4
0.2
0.0

Control

*Hesx1*$^{Cre/+}$;*Lats1*$^{fl/fl}$;
*Lats2*$^{fl/fl}$

F

Percent of AP cells

100
80
60
40
20
0

**

Control

*Hesx1*$^{Cre/+}$;
*Lats1*$^{fl/fl}$;*Lats2*$^{fl/fl}$

47.42
76.04
17.80
23.34

Ki-67

SOX9

A

TAZ

Active YAP

SOX2 / EMCN

Control

P21

*Hesx1*$^{Cre/+}$;*Lats1*$^{fl/fl}$;
*Lats2*$^{fl/+}$

B

Control

P56

*Hesx1*$^{Cre/+}$;*Lats2*$^{fl/fl}$

C

SOX2 / EMCN

Control

*Hesx1*$^{Cre/+}$;*Lats1*$^{fl/fl}$;
*Lats2*$^{fl/+}$

PL

IL

PL

IL

*

D

gamma H2A.X

Control

P56

*Hesx1*$^{Cre/+}$;*Lats1*$^{fl/fl}$;
*Lats2*$^{fl/+}$

E

p63

AE1 / AE3

Control

*Hesx1*$^{Cre/+}$;*Lats1*$^{fl/fl}$;
*Lats2*$^{fl/+}$

F

Synaptophysin

NSE

Chromogranin

Vimentin

Control

*Hesx1*$^{Cre/+}$;*Lats1*$^{fl/fl}$;
*Lats2*$^{fl/+}$

A

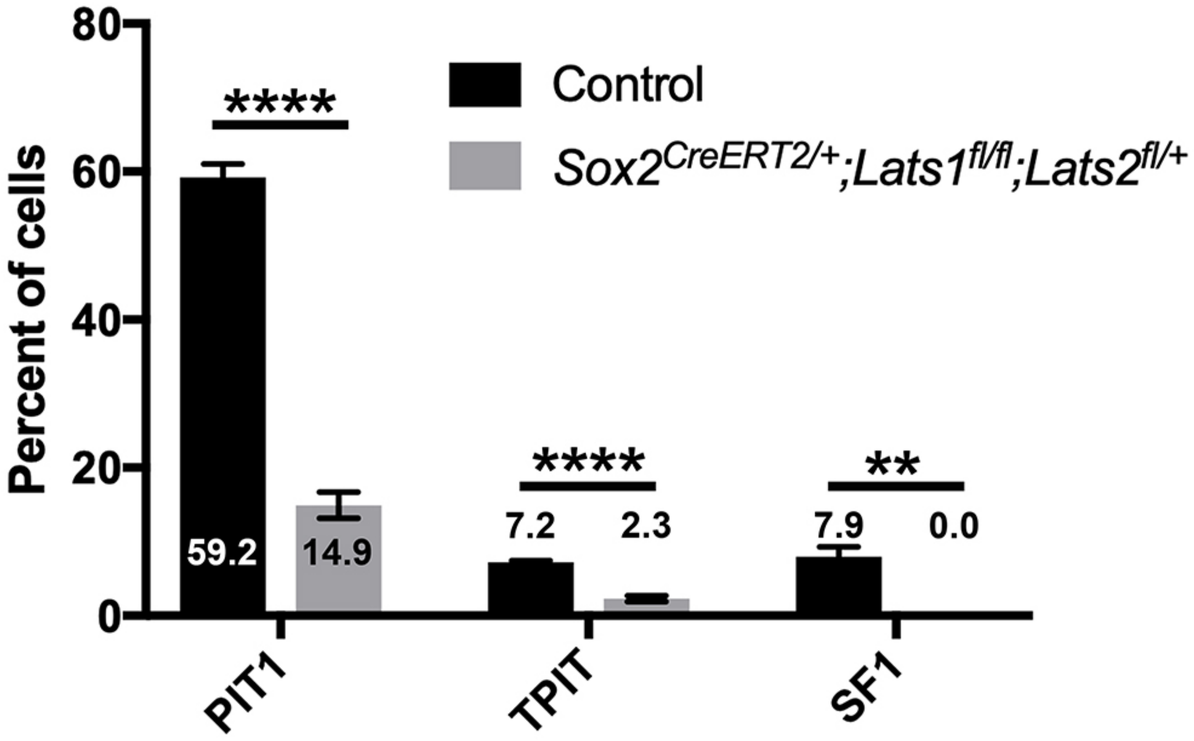
Percent of cells
80
60
40
20
0
Control
Sox2CreERT2/+;Lats1fl/fl;Lats2fl/+
****
****
**
59.2
14.9
7.2
2.3
7.9
0.0
PIT1
TPIT
SF1

B

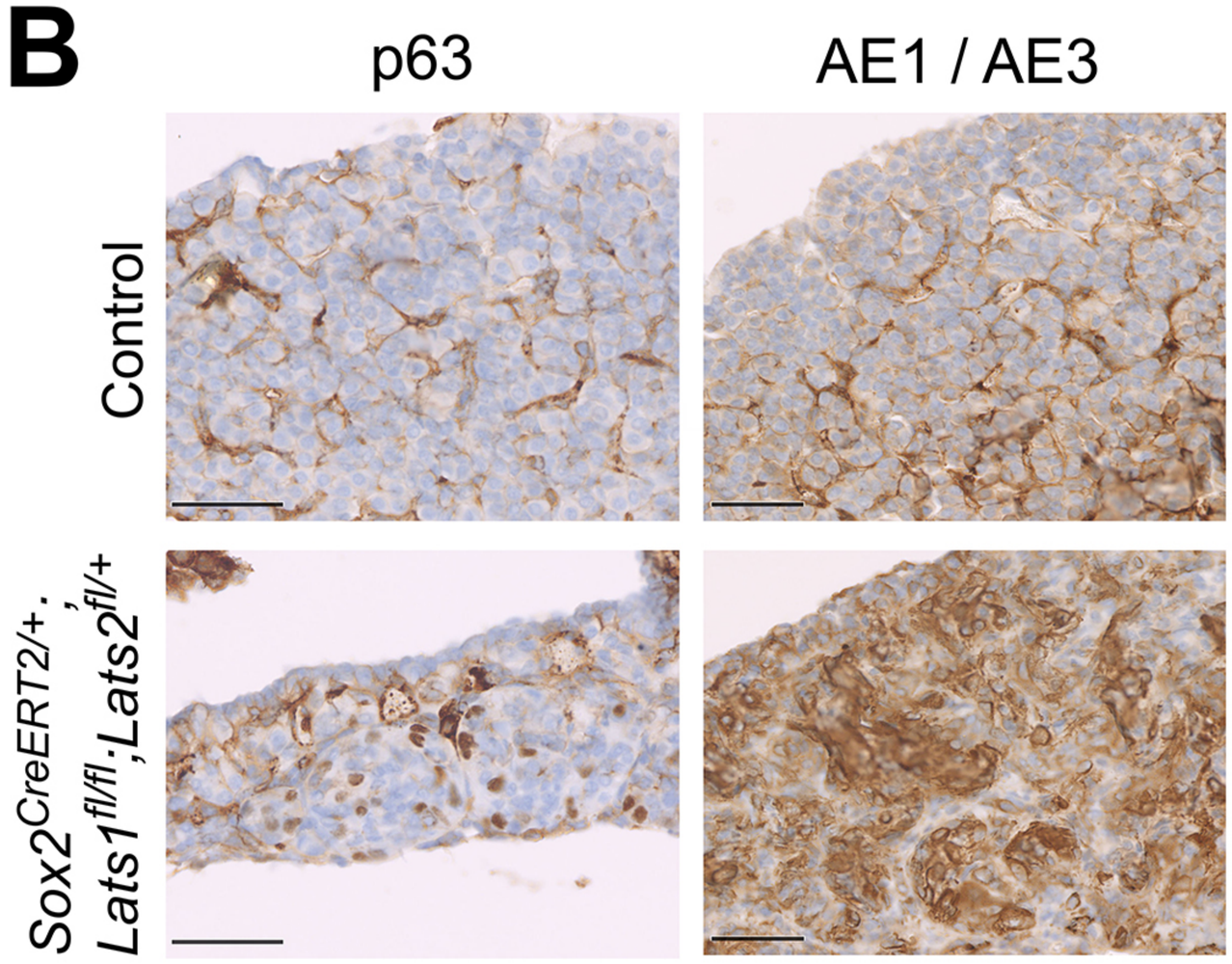
p63
AE1 / AE3
Control
Sox2CreERT2/+; Lats1fl/fl;Lats2fl/+

C


YAP / GFP
YAP
GFP
SOX2 / GFP
SOX2
GFP
Sox2CreERT2/+;Lats1fl/fl;Lats2fl/+;R26mTmG/+
(i)
(i')
(ii)
(ii')

A

Control

YAP-TetO

P42

P63

P105

B

*Cyr61*

*Ctgf*

Control

YAP-TetO

P42

C

SOX2

SOX2 / Ki-67

H&E

PIT1

Control

YAP-TetO

P105

SOX2 / SOX9

TAZ

YAP

pYAP

D

P21

P42

P63

ON DOX

OFF DOX

Control

YAP-TetO

(Recovery) P63

*Cyr61*

*Ctgf*

E

Expression (A.U.)

60

40

20

0

****

****

**

***

*Cyr61*

*Ctgf*

Control

*Hesx1*$^{Cre/+}$;*R26*$^{rtTA/+}$;*Col1a1*$^{tetO\text{-}Yap/+}$ (YAP-TetO), DOX P21-P42

*Sox2*$^{CreERT2/+}$;*Lats1*$^{fl/fl}$;*Lats2*$^{fl/+}$ P35, Tmx P5/6